Journal of Wind Engineering & Industrial Aerodynamics 228 (2022) 105076

Contents lists available at ScienceDirect

Journal of Wind Engineering & Industrial Aerodynamics

journal homepage: www.elsevier.com/locate/jweia

Comparison of Tornado-induced pressures on building from CFD model with TTU experimental measurements

Sumit Verma[a], R. Panneer Selvam[a,*], Zhuo Tang[b], Delong Zuo[b]

[a] Department of Civil Engineering, BELL 4190 Univeristy of Arkansas, Fayetteville, AR, 72701, USA
[b] National Wind Institute, Texas Tech University, Lubbock, TX, TX, 79409, USA

ARTICLE INFO

Keywords:
3D CFD simulation
Tornado-like vortex induced pressure
Building
Experimental comparison
Building size
Flow structure

ABSTRACT

Several studies have been carried out to investigate the magnitude of forces induced by tornado-like winds on buildings from experimental as well as computational side. The number of experimental studies evaluating the wind loads due to tornado-like vortices are comparatively greater in number than studies based on computational fluid dynamics (CFD). Furthermore, the limited number of CFD studies were often not validated by comparing with experimental measurements. In this work, an attempt is made to validate a CFD model by comparing the pressures induced by tornado-like vortices on a building model with experimental measurements from the tornado simulator at Texas Tech University (TTU). Results of the comparison indicate that the pressure coefficients obtained from the CFD model agree well with TTU experimental datasets. Besides, the effect of building size as well as the effect of flow structure of vortex on pressure coefficients on the building induced by tornado-like vortex is also investigated. It is observed that the pressures on the building can differ by up to 100% when different sizes of building is considered and the vortex with a single celled structure creates the most unfavorable loading conditions on the building model.

1. Introduction

Tornadoes can cause great economic distress (Changnon, 2009) as well as substantial loss of human lives (Molloy and Mihaltcheva, 2013). For this reason, exploration of tornado wind field and the pressures induced by tornadoes on buildings has gained more attention in the research community in recent years. Many field studies have been carried out in the past to explore the wind velocity field and pressure distribution of a live tornado (e.g., Bluestein and Pazmany, 2000; Alexander and Wurman, 2005; Kosiba and Wurman, 2010; Kosiba and Wurman, 2013). Field data from real-world tornadoes are the most accurate source of data on tornadoes and those datasets are helpful in analyzing the cause of failure of buildings during tornadic events. However, further engineering application of field datasets is limited by the fact that these data are mostly velocity measurements at elevations well above most buildings and pressure measurements at the ground surface. In addition, the velocity and pressure measurements often lack the resolution required for engineering applications (see Fig. 5).

Due to the limitations of field measurements, an alternative method was devised to study tornadoes by simulating tornado-like vortices in a controlled environment inside experimental tornado simulators. For this purpose, various tornado simulators were built. However, from an engineering standpoint, the major tornado simulators include the VorTECH at Texas Tech University (TTU), the ISU tornado simulator at Iowa State University (ISU) and the WindEEE dome at Western University (WU). Details about the geometric configuration and flow generation mechanism of these tornado simulators can be obtained from Tang et al. (2018a, 2018b), Haan et al. (2010) and Hangan (2014) respectively. Detailed investigation on the wind field of tornado-like vortices generated by these simulators have been carried out by Tang et al. (2018a, 2018b), Haan et al. (2008) and Refan and Hangan (2018). Similarly, investigation on the pressures and forces induced by tornado-like vortices on the building models have been carried out by Sengupta et al. (2008), Haan et al. (2010). However, experimental simulation of tornado-like vortices and induced loading on low-rise building models has its own challenges. Because tornado-like flows are highly turbulent and three-dimensional, it is challenging to measure the wind velocities at core regions of vortices with high resolution/fidelity (Tang et al., 2018a; Refan and Hangan, 2016). In addition, due to the large size of full-scale tornadoes and the limited sizes of vortices that tornado simulators can generate, it is difficult and, in some cases, even impractical to test building models at appropriate scales in tornado simulators. This is true even with the availability of the large-scale simulators constructed

* Corresponding author.
E-mail addresses: sv015@uark.edu (S. Verma), rps@uark.edu (R. Panneer Selvam), zhuo.tang@ttu.edu (Z. Tang), delong.zuo@ttu.edu (D. Zuo).

https://doi.org/10.1016/j.jweia.2022.105076
Received 22 February 2022; Received in revised form 5 June 2022; Accepted 27 June 2022
Available online 10 July 2022

Nomenclature

S	Swirl ratio
V_{tmax}	Max. tangential velocity
Ref. Vel.	Reference Velocity
r_c	Core radius
OA	Orientation Angle
C_p:	Pressure Coefficient
V@ RH	Velocity at roof height
Ref. P:	Reference pressures
$P_{max,g}$:	Max. pressure at ground
C_{fx}	Force coefficient in the X-direction
C_{fy}	Force coefficient in the Y-direction
$V_t + V_{trans}$	Sum of tangential & translational velocity
C_{fz}	Force coefficient in the Z-direction
Max. VH	Max. Horizontal Velocity
Max. V_t @ MEH	Max. tangential velocity at mean eave height
$P_{s,g}$:	Static pressure at ground surface
$P_{a,o}$:	Ambient pressure outside the tornado simulator
$P_{s,f}$	Static pressure far from tornado vortex

in recent decades (Haan et al., 2008; Refan and Hangan, 2016 and Tang et al., 2018a). In addition, some existing tornado simulators can simulate the effects of translating tornadoes. However, the ratio of translation speed to maximum mean tangential velocity of the vortices generated in the simulators often cannot match the corresponding ratios of many full-scale tornadoes (Haan et al., 2010, Refan and Hangan, 2016).

Many of the challenges in full-scale and laboratory studies can be overcome through numerical simulation based on Computational Fluid Dynamics (CFD). Early CFD work on tornado simulation were primarily based on numerical modeling of tornado-like winds by axisymmetric vortices (e.g., Harlow and Stein, 1974); Rotunno (1979). Those studies mostly entailed a qualitative comparison of the features of numerically simulated vortices with those of full-scale tornadoes or experimentally generated tornado-like vortices (e.g., Rotunno, 1979; Lewellen et al., 1997; Lewellen and Lewellen, 2007; Nolan and Farrell, 1999). In recent years, many numerical simulations have been conducted to replicate physical tornado simulators and study the tornado-like vortices simulated by the CFD models (Yuan et al., 2019; Gairola and Bitsuamlak, 2019). The numerical results are usually compared with corresponding experimental datasets before the numerical models are used to study other aspects of tornado-like flows (Ishihara et al., 2011; Liu and Ishihara, 2015; Kuai et al., 2008; Yuan et al., 2016; Gairola and Bitsuamlak, 2019; Verma and Selvam, 2021c).

There exists a substantial number of studies based on the comparison of wind field simulated using CFD with experimentally generated tornado-like vortices. However, only a limited number of numerical studies have been carried out to investigate the interaction between tornado-like flows and building models. CFD modeling to quantify the forces induced by tornado-like vortex on building was relatively unexplored until the early 2000s. Selvam and Millett (2003 & 2005) numerically simulated tornado-like vortices based on the Rankine Combined Vortex Model (RCVM) using Large Eddy Simulation (LES) and compared the force coefficients on a cubical building in tornado-like and straight-line (SL) winds. They concluded that the forces due to tornado-like winds could rise by up to 50% for walls while even higher for roof, by up to 100% in comparison to SL winds. Nasir et al. (2014) and Nasir and Bitsuamlak (2016) computed wind load on a tall building due to a single-celled tornado-like vortex using Reynolds Averaged Navier Stokes (RANS) model. They concluded that the largest suction forces are encountered by building when it is at the center of tornado-like vortex, primarily due to the large pressure drop at this location in the vortex. Yousef et al. (2018) compared the forces caused by tornado-like winds on a dome-shaped and a prism-shaped building. They concluded that the loads exerted by tornado-like winds on the dome shaped building is lesser than that on the prism-shaped building due to the differences in shape of the building models. Gairola and Bitsuamlak (2018) compared the flow field around a high-rise building obtained from Large Eddy Simulation (LES) with the results from Yang et al. (2011) and WindEEE dome. They found a good qualitative agreement between the CFD and experimental flow field. The numerical model, however, underestimated the force coefficients when compared with the experimental results. In addition, inconsistencies were also observed in moment coefficient curves obtained from numerical model when compared with the experimental results. Nonetheless, the study concluded that the largest force was encountered by the building when it is placed at the core radius of tornado-like vortex. The study also pointed out that vortex wandering can greatly influence the interpretation and comparison of wind loading on buildings due to tornado-like vortices in experimental as well as CFD tornado simulators.

Although a number of studies have been carried out both on the experimental side and using CFD, comprehensive studies (like what have been done in case of straight-line winds) that enable adequately accurate assessment of tornadic loading on buildings is lacking. A detailed literature review is also done to learn about the features of tornado-like vortex such as the core radius, the maximum tangential velocity and the swirl ratio of vortex considered in different work of literature. In addition, the scale (or size) of the building models, reference quantities (such as reference pressure and velocity) and the peak pressure coefficients on the building reported in different studies in the existing literature is also presented. The information obtained from literature review is summarized in Table 1. The nomenclature for the abbreviations used in Table 1 is listed before the 'Introduction' section. In addition, the forces and pressures induced by tornado-like winds on building are documented in Table 2. It can be readily noticed in Table 2 that there is significant variation in the reported peak forces and pressures on building due to tornado-like winds.

From review, it is observed that a diverse range of flow structure of

Table 1
Different features of tornado vortex and scale of building model used for estimating tornado forces on building.

SN	Reference	Model Scale	S	r_c	V_{tmax}	OA	Ref. Vel.
1	Selvam and Millett (2005)	–	–	60 m = 3 units	90 m/s = 4.5 units/s	0°, 45°	$V_t + V_{trans}$
2	Mishra et al. (2008)	1:3500	0.19	13 mm	–	–	Max. VH
3	Sengupta et al. (2008)	1:100	0.24, 1.14	0.3m, 0.53m	9.7 m/s	0°, 45°	Max. V_t
4	Haan et al. (2010)	1:100	0.08–1.14	0.23–0.53m	8.3–11.9 m/s	0°–90° @ 15°	Max. VH
5	Hu et al. (2011)	1:200	0.1	0.16m	10 m/s	0°–90° @ 15°	Max. V_t
6	Sabareesh et al. (2012)	–	1.3	37.3 mm	–	–	V @ RH
7	Sabareesh et al. (2013)	–	0.43, 0.87	Fully engulfed	–	–	V @ RH
8	Liu and Ishihara (2015)	1:1900	2.44	0.112m	18.6 m/s	–	Max. V_t @ MEH

*** Note: Fully Engulfed implies that the building model considered was fully engulfed inside the core of tornado vortex. Also, 0°–90° @ 15° implies that the orientation angles in the study was varied from 0° to 90° in increments of 15°.

Table 2
Tornado forces and pressures on a building from different work in the literature.

SN	Reference	Simulation Type	C_{fx}	C_{fy}	C_{fz}	C_p	Ref. P
1	Selvam and Millett (2005)	CFD	1.33	1.36	1.81	−2.82	0
2	Sengupta et al. (2008)	EXP	–	–	1.44^{C} 1.78^{TB}	–	–
3	Mishra et al. (2008)	EXP	2.4	2.45	2	−1	$P_{s,g}$
4	Haan et al. (2010)	EXP	2.7	2	4	−4.5	$P_{a,o}$
5	Hu et al. (2011)	EXP	0.8	0.6	2.75	−4.2	$P_{a,o}$
6	Sabareesh et al. (2012, 2013)	EXP	–	–	-5.5^{ST} -9.0^{RT}	−19	$P_{s,f}$
7	Liu and Ishihara (2015)	CFD	−1.2	0.9	2.2	−1.1	0
8	Nasir and Bitsuamlak (2016)	CFD	–	–	–	−2.5	$P_{max,g}$
9	Yousef at al. (2018)	CFD	1.4	−1.39	2.6	−3.5	0
10	Li et al. (2019)	CFD	0.1^{D} 1.5^{S}	-0.2^{D} -1^{S}	-2.4^{D} -8.4^{S}	-0.6^{D} -2.5^{S}	P_{atm} (101 KPa)

*** Note: C: Cube building; TB: Tall building; S: single-celled vortex; D: double-celled vortex; r: roof; ST: smooth terrain; RT: rough terrain, EXP: Experiment.

tornado-like vortex have been considered in the existing literature for evaluating forces on the building models (Refer Table 1). Different flow structures of tornado-like vortex have different wind velocity profiles and pressure distribution. So, they can result in different loading conditions on the building. Similarly, it can also be noticed that different model scales for building or alternatively different sizes of building have been considered while computing the pressures induced by tornado-like vortex on the building models. But the effect of variation of size of the building on the pressures induced by tornado-like vortex is still not understood very well. In addition, the pressure and force coefficients differ from one study to another on the experimental side whereas on the computational side, the pressures induced by tornado-like vortex lack comparison and/or validation by experiments. In the existing literature (Ishihara et al., 2011; Liu and Ishihara, 2015; Gairola and Bitsuamlak, 2019; Yuan et al., 2019), the CFD models are often validated with experimental measurements by comparing the wind field of simulated vortices. However, a one-to-one comparison of pressures induced by tornado-like vortex on the building simulated using CFD is lacking with experimental measurements. Current work tries to address the gap in existing literature by making a one-to-one comparison/validation between the pressure coefficients obtained from CFD model with the experimental datasets from VorTECH simulator at Texas Tech University (TTU). Similarly, the effect of variation of size of the building on the induced pressures is also investigated. In an earlier study carried out by Kikitsu and Okuda (2016), it was proposed that the ratio of size of the building to the size of the core radius of tornado-like vortex should be maintained less than 0.45. The proposition, however, was based on the analysis/comparison of load characteristics from experimental tornado simulator with Rankine vortex. Rankine Vortex Model is based on the idea of representing a tornado-like vortex primarily by the distribution of tangential velocity in the radial direction, but the radial and the axial velocity components are missed out in Rankine Vortex Model. So, in this work, the sensitivity of load characteristics on the building model is studied by solving the 3D Navier-Stokes (NS) equation in which all the three velocity components (radial, tangential and axial) are considered, and the details are reported. This type of investigation/analysis is not present in other work of the existing literature; thus, the current work adds to the knowledge from previous studies in the existing literature. Besides, the influence of different flow structures of tornado-like vortex on induced pressures on the building models is investigated. In previous studies such as Li et al. (2020), the interaction of a single-celled and a double-celled vortex with a dome was studied. The wind field (tangential velocity profile) obtained from the CFD model was compared with field measurements, but experimental validation of the pressures induced on dome by tornado-like vortex was lacking. In addition, the study focused on variation of induced wind loads on dome due to single-celled and double-celled vortex. However, the majority of residential housing comprises of prismatic buildings which are bluff as compared to more aerodynamic shape of domes (which also comprises only a very small subset of residential structures). Thus, in the current work, a prismatic bluff shape of building is considered. Both the mean and the minimum pressure coefficients as well as their ranges on a building model are reported, which adds further knowledge to previously reported study by Razavi and Sarkar (2018) in which only the maximum force coefficients on building due to a single-celled and double-celled vortex were reported. Besides, the induced pressures on

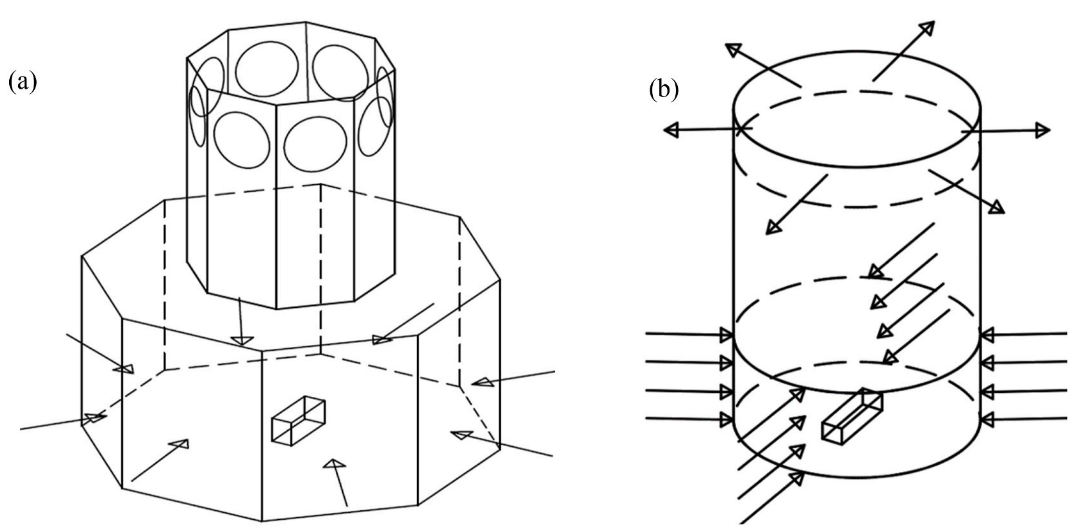

Fig. 1. (a) Experimental tornado simulator VorTECH at Texas Tech University (b) Simplified CFD tornado simulator.

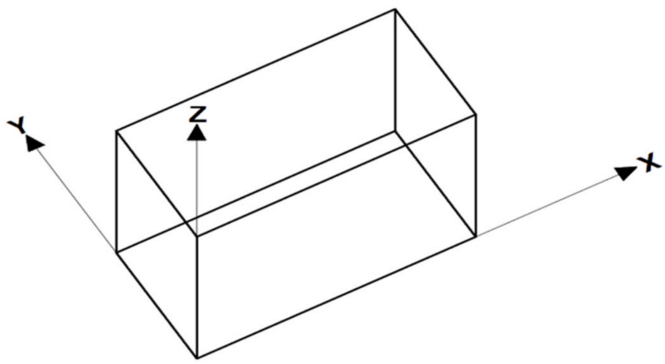

Fig. 2. 3D sketch of the building model.

the building due to a touched-down vortex is also reported in this work in contrast to previous studies, which have only focused on vortex before and after touchdown. In addition, the details of the interaction of coherent turbulent structures (suction vortices reported in detail in section 4.3) with the building model is reported in current work which is not reported previously in earlier work of literature. The interaction of coherent turbulent structures with the building is believed to be critical in developing an improved understanding of the tornado loading on buildings. Hence, in this work, an attempt is made to learn about the details as to how different flow structures of tornado-like vortices such as prior to, during and beyond touchdown differs in its interaction with a building. The differences and/or similarities in the flow features during the interaction of different flow structures of vortex with building model is also reported. Based on the discussion above, the objectives of present study are summarized below.

1.1. Objectives of current work

1. To compare and validate the pressures induced by tornado-like vortex on a building model obtained from CFD simulation with TTU experimental results.
2. To study the effect of size of the building (or differences in model scale of the building) on tornado-induced pressures.
3. To study the influence of different swirl ratio of tornado vortices (prior to, during and post-touchdown) on the induced pressures on buildings.

2. Numerical setup

2.1. Description of numerical simulator model for VorTECH facility

Fig. 1 (a) shows a 3D perspective view of a prismatic building model placed at the center of the TTU tornado simulator, and Fig. 1 (b) shows an equivalent CFD model of the experimental set up considered for this work. The inlet height of the simulator is kept at $h_o = 1$m and the updraft radius is $r_{up} = 2$m. Thus, the aspect ratio of the simulator is maintained at $a = h_o/r_{up} = 0.5$.

The outlet region provided by 8 fans of 2 ft diameter each in the TTU simulator is modeled by an effective outlet height of 0.743 m in the CFD tornado simulator. Further detail about the calculation of outlet height is provided in Verma (2022). Using the inlet height (h_o) of tornado simulator as the reference length, the effective outlet height in non-dimensional form is taken as $0.743h_o \approx 0.8h_o$. The total height of the chamber is kept as $H = 6h_o$. The dimensions of the building considered in TTU simulator is 10 cm × 5 cm x 5 cm. Accordingly, the dimension of the building model considered in the CFD model is $0.10h_o$ along the X-direction and $0.05h_o$ along the Y-direction and the Z-direction for the current study. The 3D sketch of the building considered in this work is shown in Fig. 2.

2.2. Governing equations for CFD model

The 3D Navier Stokes (NS) equation is used for flow computations. The technique of Large Eddy Simulation (LES) with Smagorinsky model is used for turbulence modeling. The continuity and momentum equations in tensorial notation is as follows:

Continuity Equation:

$$\frac{\partial \overline{U}i}{\partial x_i} = 0 \tag{1}$$

Momentum Equation:

$$\frac{\partial \overline{U}i}{\partial t} + \frac{\partial \overline{U}i\overline{U}j}{\partial x_j} = -\frac{\partial \overline{P}}{\partial x_i} + 2\frac{\partial}{\partial x_j}(\nu + \nu_{sgs})\,\overline{S}_{ij} \tag{2}$$

The variable 'ν' in Eq. (2) is the kinematic viscosity of fluid, whereas 'ν_{sgs}' is the turbulent kinematic viscosity given as

$$\nu_{sgs} = (C_{sgs}\ \Delta)^2\sqrt{2\overline{S}_{ij}\overline{S}_{ij}} \tag{3}$$

'C_{sgs}' is the Smagorinsky constant taken as $C_{sgs} = 0.1$ for the current work and 'Δ' is the cube root of the volume of a cell used in the Smagorinsky model which is given as

$$\Delta = \sqrt[3]{(\Delta x\ \ \Delta y\ \ \Delta z)} \tag{4}$$

Similarly, $\overline{S_{ij}}$ in Eq. (2) is the shear rate tensor, which is computed as

$$\overline{S}_{ij} = \frac{1}{2}\left(\frac{\partial \overline{U}i}{\partial x_j} + \frac{\partial \overline{U}j}{\partial x_i}\right) \tag{5}$$

The smallest wavelength (λ) considered in LES modeling is around $\lambda = 4h_{min}$, where h_{min} is the smallest grid spacing. In the current case, the smallest grid spacing is taken as $0.01h_o$, where $h_{o,}$ is the inlet height (1m) of the tornado simulator. Law of the wall boundary condition is implemented at the walls to capture steep velocity gradients near to the wall. The details of numerical procedure adopted for computation can be obtained from Selvam (1997) and Verma and Selvam (2021c). For this work, a semi-staggered grid used in Kashefizadeh et al. (2019) was extended for 3D modeling initially, but it led to checkerboard pressure oscillations. Thus, a staggered grid system using Control Volume Method (CVM) is used to discretize the computational domain for flow modeling. The diffusion terms of the NS equation are approximated using the Central Difference Scheme (CDS), while the convection terms are approximated using the QUICK scheme. Line iteration method is used to solve the momentum equations. The continuity equation is satisfied using the SOLA procedure from Hirt and Cook (1972). The continuity and momentum equations are solved implicitly. The Euler scheme (backward in time) is used while solving the equations and the Courant-Friedrichs-Lewy (CFL) condition is maintained by keeping the Courant number less than unity for stability of numerical scheme. The reference values considered for non-dimensionalization of the NS equation are (a) the inlet height for length scale and (b) the radial velocity at inlet height (V_{ro}) for velocity. The details about the conversion of dimensional form of NS equations to non-dimensional form can be obtained from Cengel and Cimbala (2014). All the simulations were run for a total non-dimensional time of 30 units with a non-dimensional time step size of $t^* = 0.001$. A grid size of 157 × 157 x 134 with 3,302,966 nodes based on an orthogonal grid system is used for discretization of the flow region.

2.3. Boundary conditions

A logarithmic velocity profile is used to model the inlet velocities in the X- and Y- directions in the CFD simulator. The axial profile of the mean tangential and radial velocity from Tang et al. (2018a) shows logarithmic variation for radial and tangential velocity components, thus, a log profile variation for inlet velocity was chosen for the current

Table 3
Different Grids considered for Mesh Convergence Study with their mesh sizes.

Grids	Mesh-A	Mesh-B	Mesh-C
Grid points in X-direction	101	91	177
Grid points in Y-direction	101	91	177
Grid points in Z-direction	151	81	165
Total no. of grid points	1540351	670761	5169285
Smallest size of grid	$0.04h_o$	$0.010h_o$	$0.008h_o$
Largest size of grid	$0.04h_o$	$0.050h_o$	$0.040h_o$

work. The vertical velocity component is considered zero throughout the inlet height. The maximum normalized radial velocity is taken as V_r ($z = h_o$) $= V_{ro} = 1$, and the corresponding tangential component is designated as V_{to}. The distribution of radial velocity from the base of tornado simulator (ground surface) up to the inlet height is expressed as a function of elevation (measured from the base of simulator) and is given as

$$V_r\ (z) = C_1 \ln\left(\frac{z + z_o}{z_o}\right) = C_1 \ln\left(1 + \frac{z}{z_o}\right) \tag{6}$$

The swirl ratio (S) for flow is calculated similar to Verma and Selvam (2021a) and is given by

$$S = (V_{to} / V_{ro}) / \left(2\left(h_o / r_{up}\right)\right) \tag{7}$$

Using the definition of 'S', the tangential component of velocity is obtained as

$$V_t\ (z) = 2\ \ V_r(z)\ \ S\ \ \left(\frac{h_o}{r_{up}}\right) \tag{8}$$

For the outlet velocity boundary condition, a uniform normal velocity is provided at outlet and is equal to total inlet velocity. Other velocity components are calculated in the flow domain considering their normal derivatives to be zero. No-slip boundary condition is implemented at the side, bottom, and top walls. The roughness parameters used in the model are $z_o = 0.00004h_o$ and $C_1 = 0.0924V_{ro}$. The Reynolds number considered for flow computation is 2.755×10^5, which is calculated based on the flow at the location of updraft radius and at the elevation of inlet height. The building is modeled inside the computational domain by identifying the start and end index for a building in the X, Y and Z-directions. No-slip boundary condition for velocity and zero gradient for pressure are implemented on the faces of the building model.

2.4. Grid independence study

Three different mesh (Mesh-A, Mesh-B and Mesh-C) were considered to study the effect of grid resolution on the wind field of tornado-like vortex in the CFD tornado simulator. The following were considered for 3 grids, i.e., (a) a uniform mesh (b) non-uniform mesh with stretching cells from the center of CFD simulator and (c) a hybrid mesh consisting of uniform mesh up to a distance of $0.78r_c$ from the center of simulator followed by stretching cells. The smallest and the largest grid spacing considered for the three different grids include the total number of grid points is documented below in Table 3. Similarly, the plots comparing pressure profile and tangential velocity profile from the three different grids are shown in Fig. 3. Further details about the study can be obtained from Verma (2022).

A grid independence study was carried out by comparing the ground pressure profile as well as the tangential velocity profile in the horizontal XY-plane at an elevation of $z = 0.01h_o$ between the grids. The pressure profile obtained from Mesh-A and Mesh-B are compared with the profile from Mesh-C and it is found that the normalized root mean squared error (NRMSE) for Mesh-A is about 13.51% and 15.48% for Mesh-B. Similarly, after comparing the tangential velocity profile from Mesh-A and Mesh-B with that of Mesh-C, the NRMSE is found to be 7.23% for Mesh-A and 41.46% for Mesh-B. From Table 3, it can be observed that Mesh-B is very coarse as compared to Mesh-A and Mesh-C. So, the NRMSE in both the tangential and pressure profiles are high for Mesh-B. For Mesh-A and Mesh-C on the other hand, the NRMSE value for pressure is slightly higher than 10% whereas for tangential velocity profile, it is less than 10%. From these observations, it is concluded that the obtained solution from Mesh-A & Mesh-C is grid independent and thus, Mesh-C (the finest of all the 3 grids) is used for further computations, analyses and experimental validation unless otherwise stated.

3. Methodology

In this work, the CFD tornado simulator model from Verma and Selvam (2021c) was extended to study the interaction of tornado-like vortex with a building. For this work, the experimental tests were carried out on several specimens of building model in the TTU simulator. For the ease of naming, the specimens of different building model are referred to as VorTECH Chamber Building Model-1 (VCBM1), VCBM2, etc. From the different building models considered in TTU simulator, the building model of size 10 cm × 5 cm x 5 cm is used for validation of CFD model and is designated as VCBM1 for this work. In section 4.1 below,

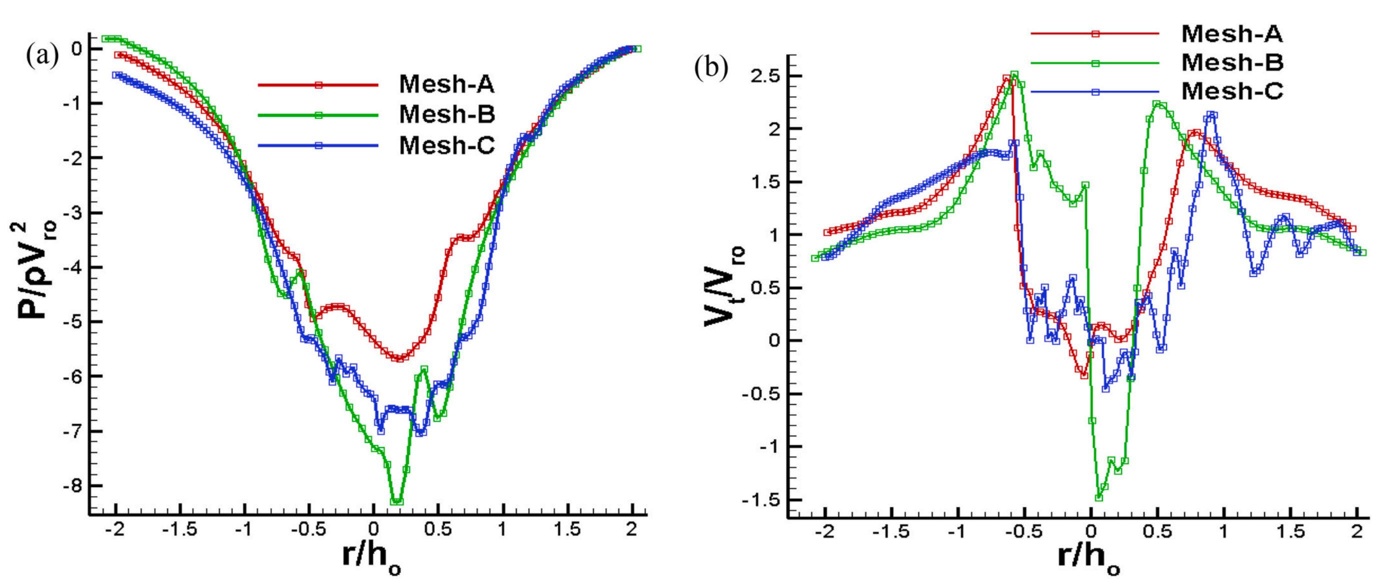

Fig. 3. Comparison of (a) ground pressure profile (b) tangential velocity profile between 3 grids at the horizontal.

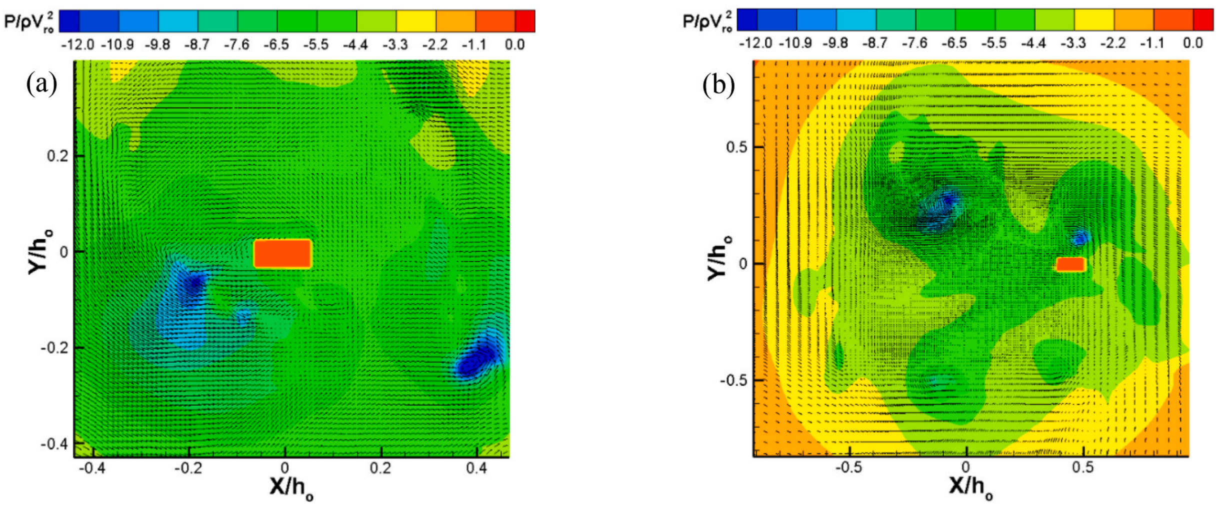

Fig. 4. Pressure contour plot around the building in XY-plane at $z/h_o = 0.01$ when building is placed at (a) center of tornado chamber ($r/h_o = 0$) (b) core radius location ($r/h_o = 0.46$).

the details about the validation of mean C_p contour on VCBM1 are covered. For experimental validation, the same building VCBM1 is considered in the CFD model as in the TTU simulator and the building is subjected to a double-celled vortex of $S = 0.83$. The computed pressure coefficients are then validated by experimental datasets, specifically by comparing the mean C_p contour on VCBM1 and the mean C_p profile along the centerline of VCBM1.The experimentally validated case of VCBM1 is then treated as the base case for two other studies that follow in section 4.2 and 4.3. In section 4.2, the effect of variation of size of the building on induced pressures is studied. For this work, the building VCBM1 (used in experimental validation) is considered as one of the buildings and for the other building, a slightly larger building of size $0.10h_o$ x $0.10h_o$ x $0.10h_o$ (designated as building2) is considered. In section 4.3, the effect of different flow structures of vortex on the induced pressures is studied. For this work, three different swirl ratios of vortex (i.e., $S = 0.15$, 0.36 & 0.83) are considered, which are representative cases of a single-celled vortex before touchdown, a touched-down vortex, and a double-celled vortex beyond touchdown respectively. For all these work, two cases are considered, i.e., (a) when the building is placed at the center of vortex ($r/h_o = 0$) and (b) when the building is placed at the core radius of vortex ($r/h_o = 0.46$).

4. Results

4.1. Comparison of Tornado-induced pressures on building from CFD model with TTU experimental data

Even though full-scale tornadoes are translating in nature, the interaction of wind field of a stationary tornado-like vortex with building placed at different locations can still provide valuable insights on the flow physics and forces induced by tornado-like vortex on a building. This is because the interaction of a stationary tornado-like vortex with building can still be viewed as the interaction with a translating tornado-like vortex at some particular time instant.

Therefore, in this section, the induced pressures on the building from CFD model are computed and compared/validated by TTU experimental measurements. The pressure contour plot around the building when it is placed at the center and at the core radius of tornado-like vortex is shown in Fig. 4. To estimate the wind loads due to a stationary tornado wind field interacting with the building model, which is placed at different radial locations of the tornado simulator, the values of pressure coefficient (C_p), is computed as per Eq. (9).

$$(C_P) = \frac{(P - P_{ref})}{0.5\ V_{t,max}^2} = \frac{\left(P^* - P_{ref}^*\right)\ V_{ro}^2}{0.5\ V_{t,max}^{*2} V_{ro}^2} = \frac{\left(P^* - P_{ref}^*\right)}{0.5V_{t,max}^{*2}} \tag{9}$$

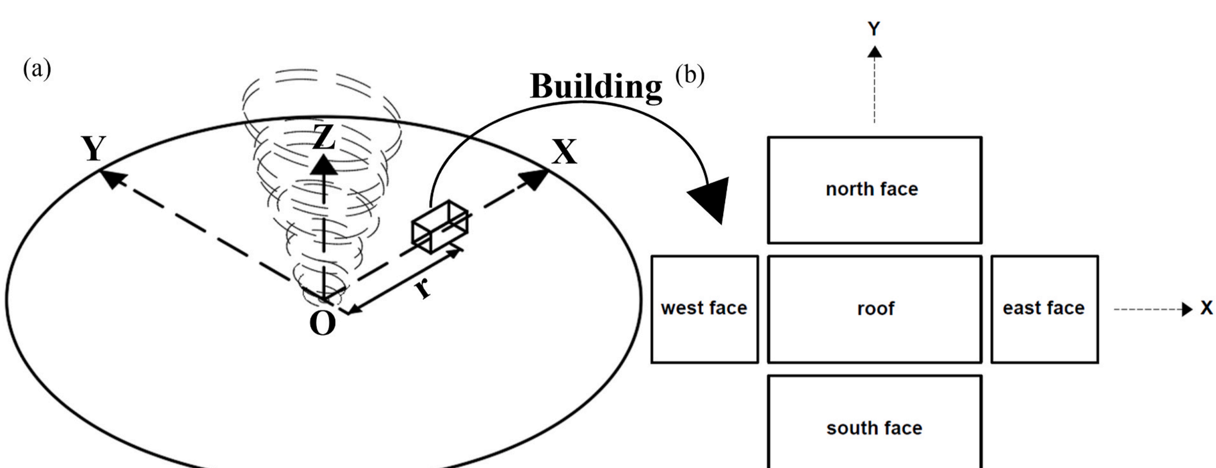

Fig. 5. (a) Schematic diagram of interaction of tornado wind field with the building when it is placed at different radial locations (r) along the X-axis (b) Exploded view of the faces of building.

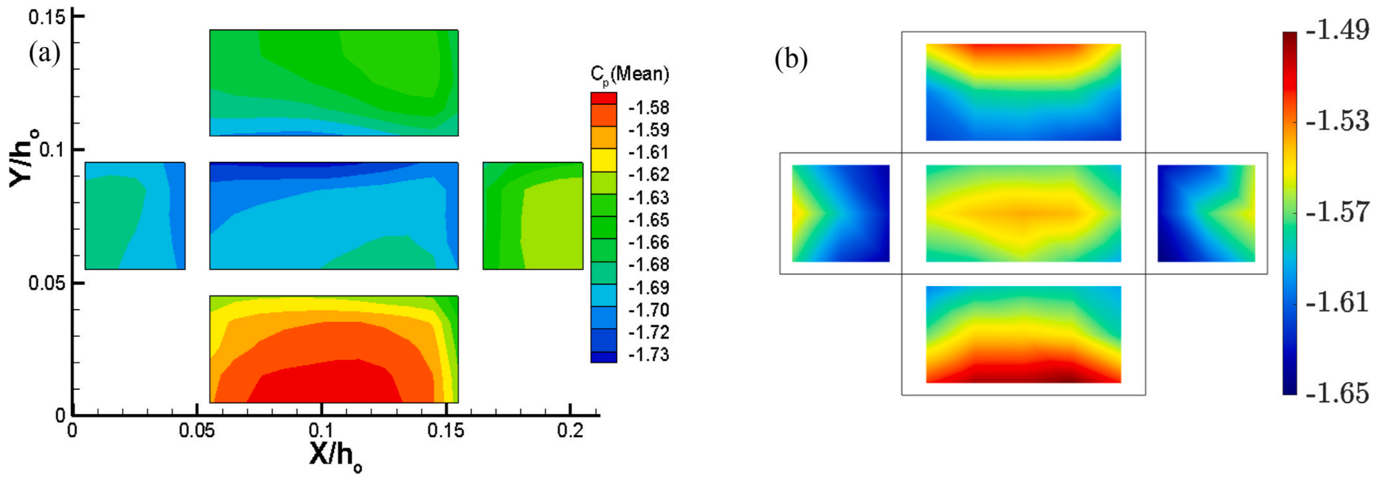

Fig. 6. Comparison of mean C_p contour for swirl ratio (S) = 0.83 and aspect ratio (a) = 0.5 when building is placed at the center of tornado chamber (a) CFD (b) TTU Experiment (11 × 6 x 6 grid for building).

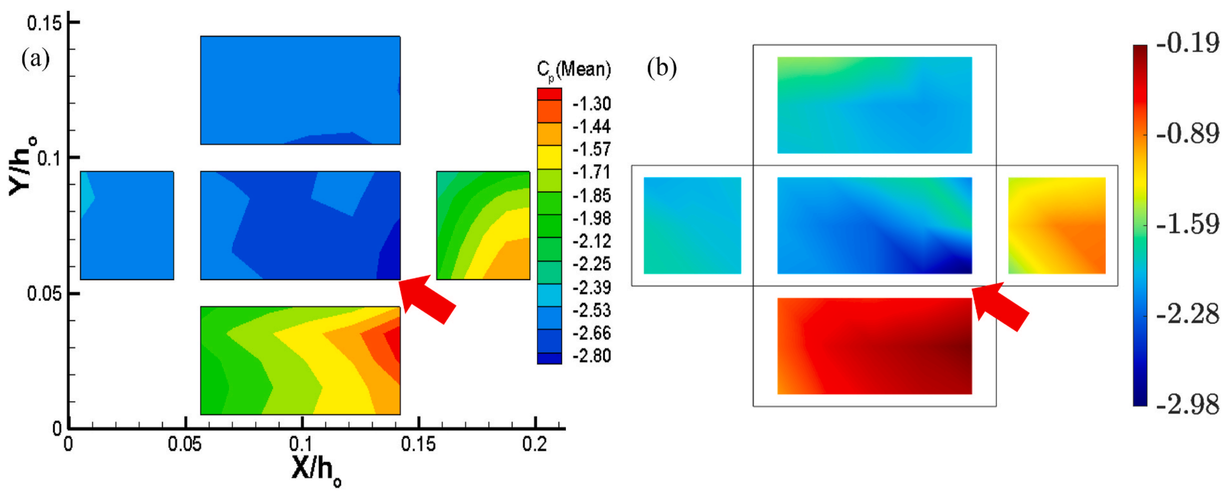

Fig. 7. Comparison of Mean C_p contour for swirl ratio (S) = 0.83 and aspect ratio (a) = 0.5 when building is placed at the location of core radius (r_c/h_o = 0.46) of tornado vortex for S = 0.83 (a) CFD (b) TTU Experiment (11 × 6 x 6 grid for building).

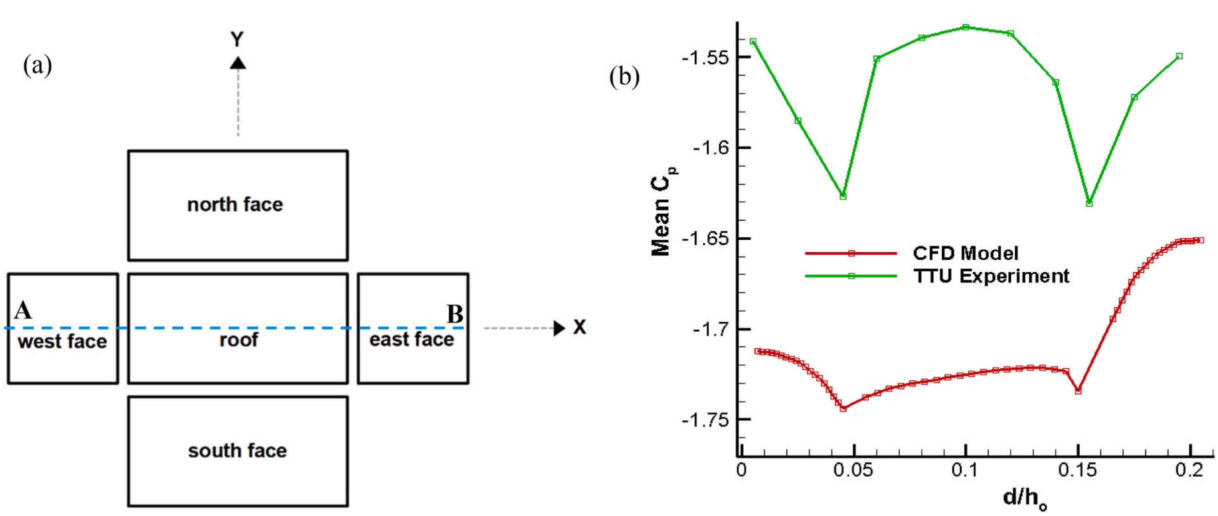

Fig. 8. (a) Demonstration of centerline AB along which mean C_p profile is extracted (b) Comparison of Mean C_p profile along the centerline of building 'VCBM1' between the CFD model and TTU experiment for S = 0.83 when the building is placed at the center of CFD tornado simulator.

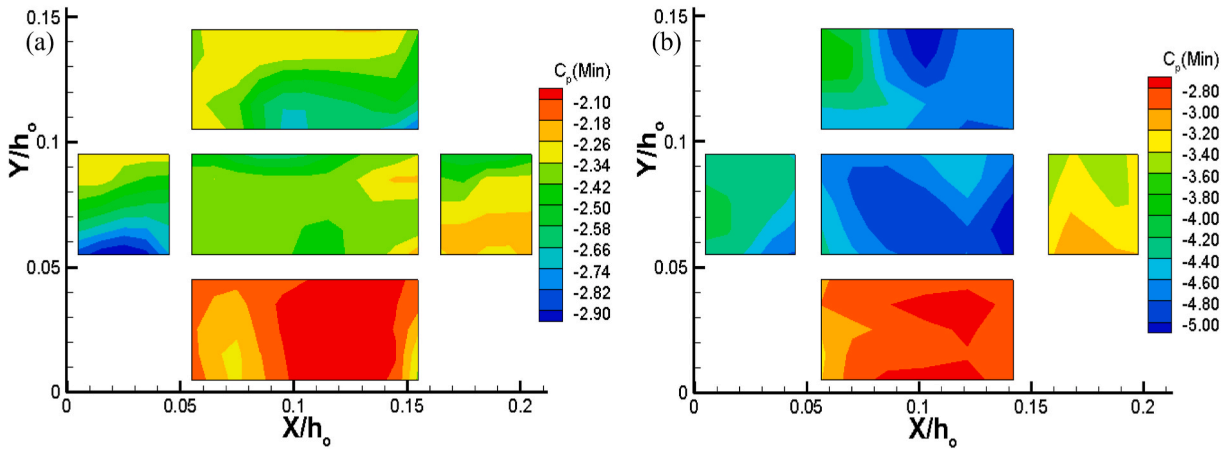

Fig. 9. Comparison of the minimum C_p on the faces of building for $S = 0.83$ when the building is placed at (a) the center of CFD tornado simulator (b) the core radius of tornado-like vortex.

4.1.1. *Pressure contour on building for different radial location of building from center of Tornado simulator*

The schematic diagram of a tornado-like vortex interacting with building placed at different radial locations from the center of vortex and the exploded view of the building is shown in Fig. 5. The values of mean pressure coefficient on the faces of the building show reasonable agreement between the CFD model and the TTU experimental datasets in Fig. 6. When the building is placed at the center of CFD tornado simulator, the mean C_p values range from −1.58 to −1.73, whereas that for TTU experiment, the corresponding C_p values range from −1.49 to −1.65. The pressure coefficients predicted by the CFD model shows deviation from the experimental datasets by about 5.4% on average. Overall, the values obtained from CFD agree reasonably with the TTU experimental datasets except for some discrepancy, which may be due to slight variation in the magnitude of maximum mean tangential velocity, which is used for computing the pressure coefficient (C_p). As C_p depends on the square of maximum mean tangential velocity (V_{tmax}), so even a slight variation in V_{tmax} can strongly affect the values of C_p. Applying the same reasoning, it is suspected that the slight variation between the CFD results and TTU datasets may have occurred (see Fig. 6).

For the case when the building is placed at the location of core radius (Fig. 7), a good qualitative agreement in the C_p contour values can be noticed readily again. The minimum of mean C_p occurs on the south-east corner of the roof (pointed by arrow pointers) with a magnitude of about −2.8 for CFD model whereas for TTU experiment, the minimum of mean C_p is about −2.98 at tentatively the same location as the CFD model. However, the range of pressure variation is different between the CFD model and TTU experiment; the range of mean C_p varies between −1.3 and −2.8 for the CFD model whereas for TTU experiment, the range varies between −0.19 and −2.98. Considering the maximum negative C_p, the deviation in magnitude of C_p predicted by the CFD model in comparison to TTU experiment is about 6%. However, there are inconsistencies in the minimum negative C_p predicted by the CFD model as compared to TTU experiment. At the location of core radius, the grid resolution decreases as the cells start stretching. It is suspected that lower grid resolution at the location of core radius might have caused the discrepancy in range of pressure coefficients between the CFD model and TTU experiment.

As shown in Fig. 8 (a), an attempt is made to extract the mean C_p profile along the centerline of the building (i.e., along line AB). After extracting mean C_p along the centerline of the building, the profile obtained from CFD model is compared with TTU experiment in Fig. 8(b). The normalized root mean squared error (NRMSE) between the two profiles is computed and it is obtained as 9.11%. After analyzing the mean pressure contours both qualitatively and quantitatively, it is concluded that the CFD model can give a reasonable prediction of TTU experimental flow field and induced pressures on the building model.

During tornadic events, usually the roofs are blown off due to static pressure drop caused by tornadoes, so, it would be of engineering significance to determine the minimum values of C_p when the building is placed at different radial locations with respect to the center of tornado-like vortex. In Fig. 9, the C_p contour plots of the minimum pressure obtained from CFD model are plotted when building is placed at two different radial locations, i.e., at $r/r_c = 0$ in Fig. 9(a) and $r/r_c = 1$ in Fig. 9 (b). From the contour plots, it is deduced that the roof region and wall to roof connection are indeed the most critical parts of a building which encounters enormous magnitude of suction forces on them (−2.9 in Fig. 9 (a) and −5.0 in Fig. 9 (b)) resulting in uplifting of roof and breach of the building envelope.

The pressure coefficients on the faces of building show reasonable agreement between the CFD model and the TTU experiment with an average percentage error of about 5.5% in the range of mean C_p for building placed at the center of simulator. Also, the NRMSE is about 9.11% between the mean C_p profile from CFD model and the TTU experiment, thus, the CFD model is reasonably validated with TTU experiment. The validated CFD model is used as the base case for other work in section 4.2 and section 4.3 unless otherwise stated. Furthermore, the study also shows that the roof region and parts of the building comprising of roof to wall connections are the most vulnerable parts of the building and susceptible to damage.

4.2. *Effect of size of the building on pressure coefficients using CFD model*

In section 1 (Table- 1), it can be observed that different scales (or sizes) of building models are used to evaluate pressures on the building due to tornado-like vortex in different work of literature. Different sizes or scale of buildings used to quantify wind loads on the building can affect the magnitude of induced pressures and forces on building. Alrasheedi and Selvam (2011) studied the influence of plan area of a building on induced wind forces by tornado-like vortex and observed that the vertical uplift forces on the roof of building decreases with increase in plan area of the building. Similar conclusion was drawn by Selvam and Gorecki (2012) after studying the forces produced on a 2D cylinder using different sizes of tornado-like vortex. It was evident from these studies that the size of building relative to a tornado-like vortex can influence the interpretation of induced pressures and forces on the building. But any guideline for selecting the size or scale for a building model was not provided. In that regard, Kikitsu and Okuda (2016) used different sizes/scale of building model in experimental tornado simulator at Building Research Institute (BRI), Japan, and concluded that different sizes/scale of building results in different pressures and force coefficients. They also proposed the idea of equivalent radius (r_{eq} =

Table 4
Comparison of range of the mean and the minimum pressure coefficient on the building of different sizes.

Building Size	$r/h_o = 0$				$r/h_o = 0.46$			
	Mean C_p		Min. C_p		Mean C_p		Min. C_p	
	Min.	Max.	Min.	Max.	Min.	Max.	Min.	Max.
$0.10h_o$ x $0.05h_o$ x $0.05h_o$	−1.25	−0.96	−3.00	−2.03	−2.89	−1.20	−5.22	−2.65
$0.10h_o$ x $0.10h_o$ x $0.10h_o$	−2.30	−2.05	−7.33	−3.57	−2.58	−1.45	−6.79	−2.56

$\sqrt{BD}/\sqrt{\pi}$), which is the radius for a circle whose area is equivalent to the plan area (BD) of the structure. The ratio (R_r), which is defined as the ratio of size of the building relative to the core radius of tornado-like vortex was computed using (10).

$$R_r = \frac{1}{r_c}\sqrt{\frac{BD}{\pi}} \tag{10}$$

Based on Eq. (10), Razavi and Sarkar (2018) and Alipour et al. (2020) have selected the scale of building model in their work. Kikitsu and Okuda (2016) proposed to use the ratio R_r less than 0.45 based on the comparison of load characteristics from experimental tornado simulator with Rankine vortex. However, it is pointed out that Rankine vortex models a tornado-like flow primarily by the distribution of tangential velocity profile. But it is also well-understood now that the wind field of tornado-like vortex comprises of all the 3 components, i.e., radial, tangential, and axial velocity components. The contribution of radial and axial velocity component is missed out in the Rankine vortex model. So, it might affect the proposition to use an effective ratio (R_r) of 0.45 or less while evaluating the loads induced by tornado-like vortex on the buildings, thus, limiting the scope of the proposition. Therefore, in this work, the effect of all the three velocity components on the wind field and on the induced pressures on building is accounted for by solving the 3D Navier-Stokes (NS) equation. Two different sizes of building (i.e., VCBM1 of size $0.10h_o$ x $0.05h_o$ x $0.05h_o$ used in section 4.1 & building 2 of size $0.10h_o$ x $0.10h_o$ x $0.10h_o$) are considered to learn about the differences in magnitude of induced pressures on the building when the same tornado-like vortex ($S = 0.83$) interacts with building of different sizes. In addition, the range of C_p (max. C_p – min. C_p) for both the mean and the minimum pressure coefficient is reported for two cases, viz. (a) when the building is located at the center of tornado simulator ($r/h_o = 0$) and (b) when the building is located at the core radius of tornado simulator ($r/h_o = 0.46$). The pressure coefficients for all the different cases are included below in Table 4.

For VCBM1, the scale ratio computed using Eq. (10) is 0.087 and for building2, the scale ratio is 0.123, which are both less than the critical value suggested by Kikitsu and Okuda (2016). When the building is placed at the center of CFD simulator, the range of mean C_p varies from −1.25 to −0.96 for VCBM1 whereas for building2, the range of mean C_p varies from −2.30 to −2.05. From Table 4, it can be observed that the range of mean pressure coefficient is almost the same for both the sizes of building when the building is located at the center of CFD tornado simulator. However, the absolute value of mean C_p is roughly about 2 times for building2 as compared to VCBM1. Similar trend is observed for the minimum pressure coefficient when the building is placed at the center of CFD tornado simulator. The range of minimum C_p varies from −3.00 to −2.03 for VCBM1 whereas for building2, the range of mean C_p varies from −7.33 to −3.57, which is roughly twice the values for VCBM1. This observation indicates that the induced pressures on the building can differ by about 100% when the building of different sizes or scales are used in a tornado simulator with all the relevant flow conditions remaining constant even when the ratio (R_r) is significantly lower than the critical value of 0.45. Thus, it seems that maintaining a ratio (R_r) of less than 0.45 (or significantly lower than 0.45) may not be a sufficient criterion to eliminate the effect of the size or scale of a building model on pressure induced by a tornado-like vortex.

For the case when the building is placed at core radius, the range of mean and the minimum C_p shows some variation; however, the absolute value of mean and the minimum C_p generally do not differ by a large margin. The absolute value of mean and the minimum C_p varies roughly about 3%–30% in Table 4. So, it seems like the influence of size of the building on induced pressures is more pronounced when the building is fully engulfed inside the core of tornado-like vortex rather than when it is located at the outer core (core radius) of tornado-like vortex. The distribution of mean C_p on the faces of building of both the sizes when it is located at the center and the core radius of vortex are included in Figs. 10 and 11 whereas that of the minimum pressure distribution on the building faces are included in Figs. 12 and 13.

Finally, the values of mean pressure coefficient (C_p) along the centerline of the building is plotted along the Y-axis whereas the corresponding distances (d) is plotted along the X-axis for both the buildings in Fig. 14. It can be noticed clearly that the size of building can

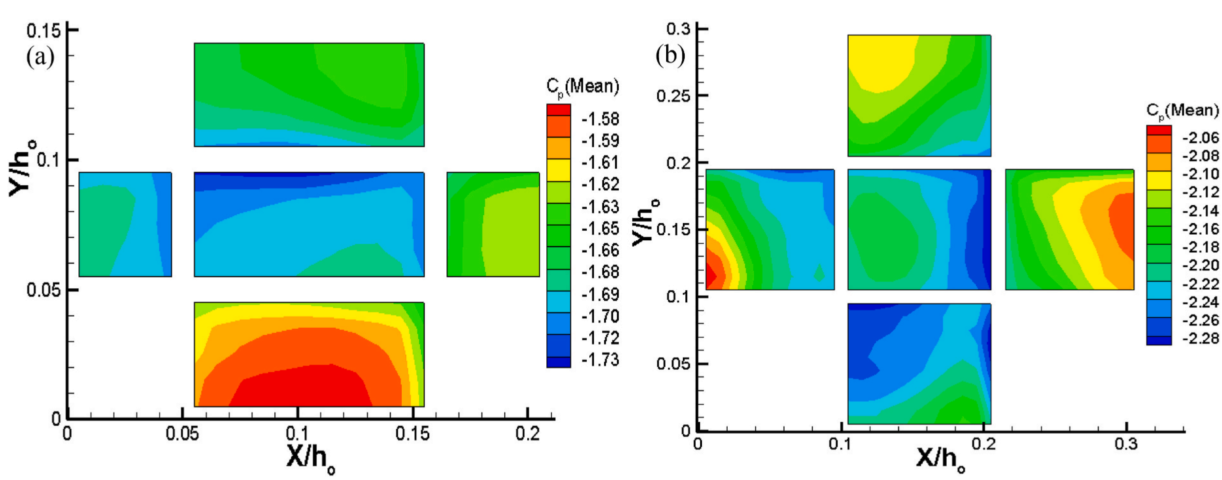

Fig. 10. Comparison of mean C_p on the faces of building for $S = 0.83$ and aspect ratio (a) = 0.5 when the building is placed at the center of CFD tornado simulator (a) VCBM1 (b) building2.

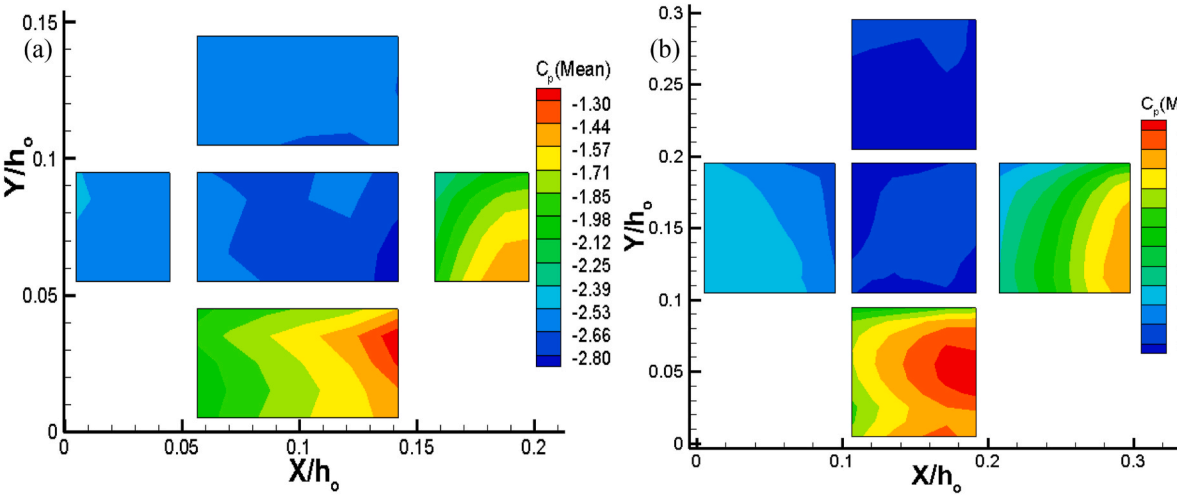

Fig. 11. Comparison of Mean C_p on the faces of building when the building is placed at core radius ($r_c/h_o = 0.46$) for S = 0.83 and aspect ratio (a) = 0.5 in CFD tornado simulator (a) VCBM1 (b) building2.

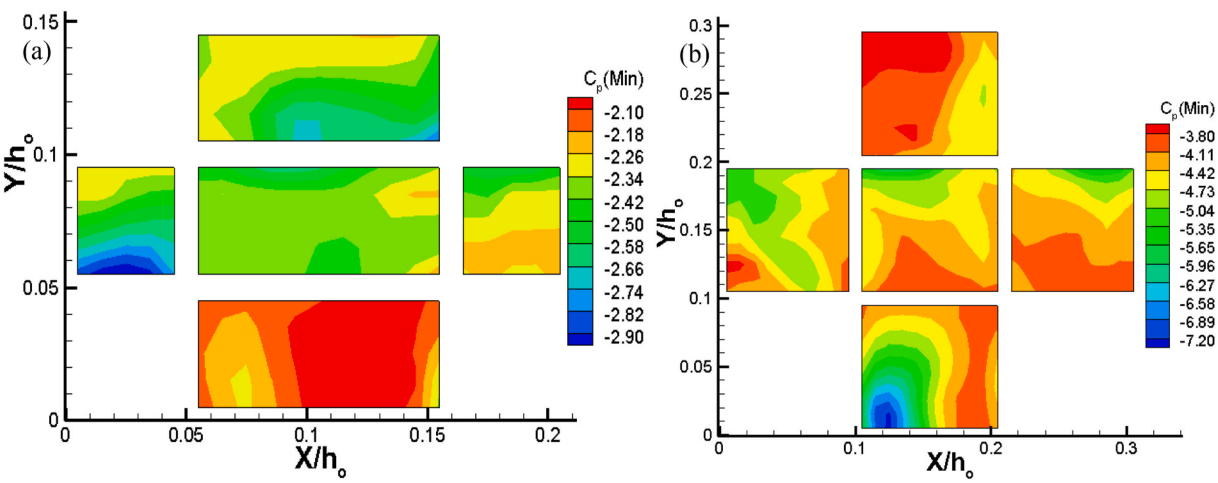

Fig. 12. Comparison of minimum C_p on the faces of building for S = 0.83 and aspect ratio (a) = 0.5 when the building is placed at the center of CFD tornado simulator (a) VCBM1 (b) building2.

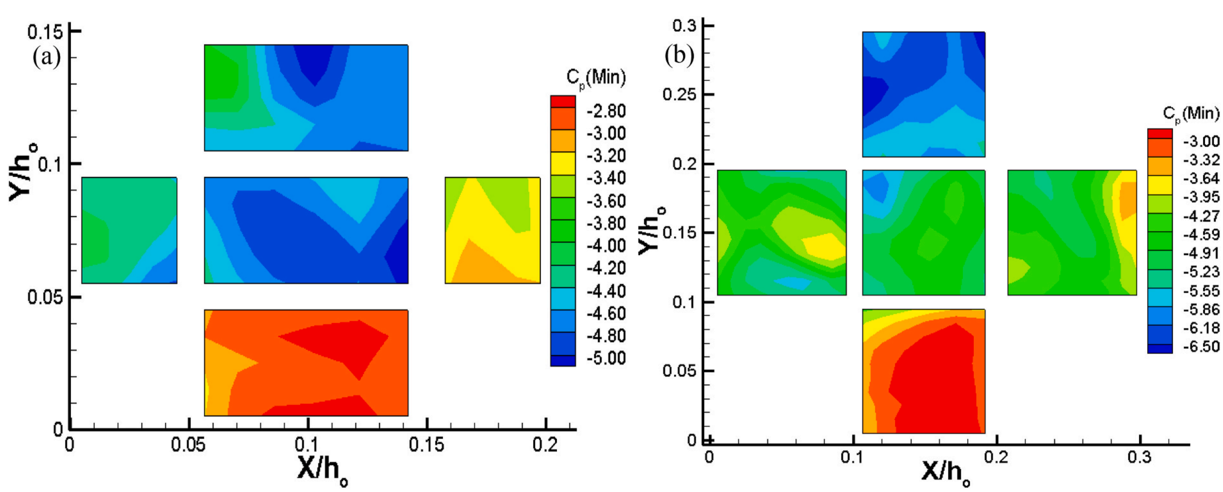

Fig. 13. Comparison of Minimum C_p on the faces of building when the building is placed at core radius ($r_c/h_o = 0.46$) for S = 0.83 and aspect ratio (a) = 0.5 in CFD tornado simulator (a) VCBM1 (b) building2.

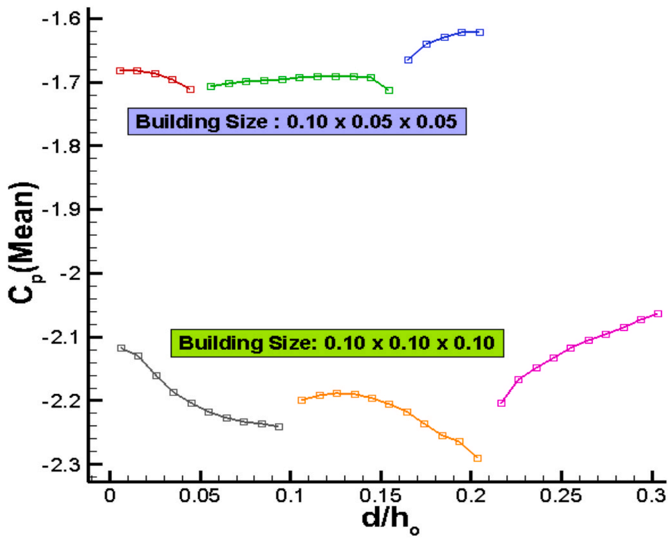

Fig. 14. Comparison of Mean C_p profile along the centerline frame of building of two different sizes.

influence the pressures induced by tornado-like vortex on the building. For VCBM1, the pressure coefficient on the westward face is about −1.7 whereas the corresponding C_p value for building2 is roughly around −2.2. Considering these two values of C_p, the induced wind load on the westward face of the building increases roughly about 25% for building2 and similar trend can be observed for roof as well as the eastward face. Hence, it seems critically important to consider an appropriate benchmark for size and scale of the building while determining tornado-induced wind pressures on building.

4.3. Effect of different swirl ratios of Tornado-like vortex on induced pressures using CFD

Different flow structures of tornado-like vortex (such as a vortex before, during and after touchdown) have different velocity profiles and pressure distribution. So, the interaction of tornado-like vortex having different flow structures is likely to produce different loading conditions on a building. Different work in the literature have considered different swirl ratios (or different flow structures of tornado-like vortices) while evaluating the pressures and forces on a building. Furthermore, the definition of swirl ratio also varies from one work of literature to another as pointed out by Gillmeier (2019). So, the value of swirl ratio calculated using different definitions/expressions could lead to further disparity in flow structure of tornado-like vortices from different work. Verma and Selvam (2021b) tried to connect different definitions/expressions of swirl ratio and then compare the flow structure of tornado vortices in different tornado simulators using a consistent definition/expression of swirl ratio. They observed that different flow structures of tornado-like vortex might exist in different tornado simulators at similar value of swirl ratio if a consistent definition is not followed. This may further lead to disparity in induced pressures during the interaction of tornado-like vortex with buildings. The experimental study carried out by Razavi and Sarkar (2018) examined the forces induced by tornado-like vortex on a building due to a single-celled tornado-like vortex (S = 0.16) as well as a two-celled tornado-like vortex (S = 0.86) and concluded that the former produced larger peak loads on a building compared to two-celled tornado-like vortex. They also observed that the horizontal drag and vertical lift forces occurred on the building concurrently. They concluded that the simultaneous occurrence of horizontal drag and vertical lift could be a significant contributing factor for loads induced by tornado-like vortex on the building model. Similarly, Li et al. (2020) used CFD simulation to investigate the loads induced by a single-celled and a double-celled tornado-like vortex on a dome-shaped building. They concluded that a single-celled tornado vortex could produce peak load on a dome-shaped building than a double-celled vortex. However, they also speculated that a double-celled vortex could cause dynamic loading effect on the dome due to rapidly fluctuating forces over a short interval of time. Different flow structures of tornado-like vortex can lead to different magnitude of vortex induced pressures and forces on building. However, there are no guidelines in the existing literature and/or building codes that provides recommendation for selecting a particular flow structure (or swirl ratio) of vortex for load estimation and building design purposes in tornado-prone areas. Besides, the studies mentioned above are mostly based on comparison of vortex-induced forces on building between a single-celled and a double-celled tornado-like vortex. However, the kind of vortex (or the flow structure) that would be suitable for developing wind load provisions for load calculation and design of buildings in tornado-prone areas is not generally identified or suggested. Thus, in this work, a systematic investigation is carried out to quantify the pressures induced on a building model by different flow structures of a tornado-like vortex. The swirl ratio of tornado-like vortex is gradually varied from a low value to a higher value (i.e., S = 0.15, 0.36 and 0.83, which are representative of vortex before, during and after touchdown respectively) and its effect on induced pressure on the building model is discussed. Similarly, the differences in flow features in the vicinity of building model resulting due to the interaction of different flow structures of vortex is

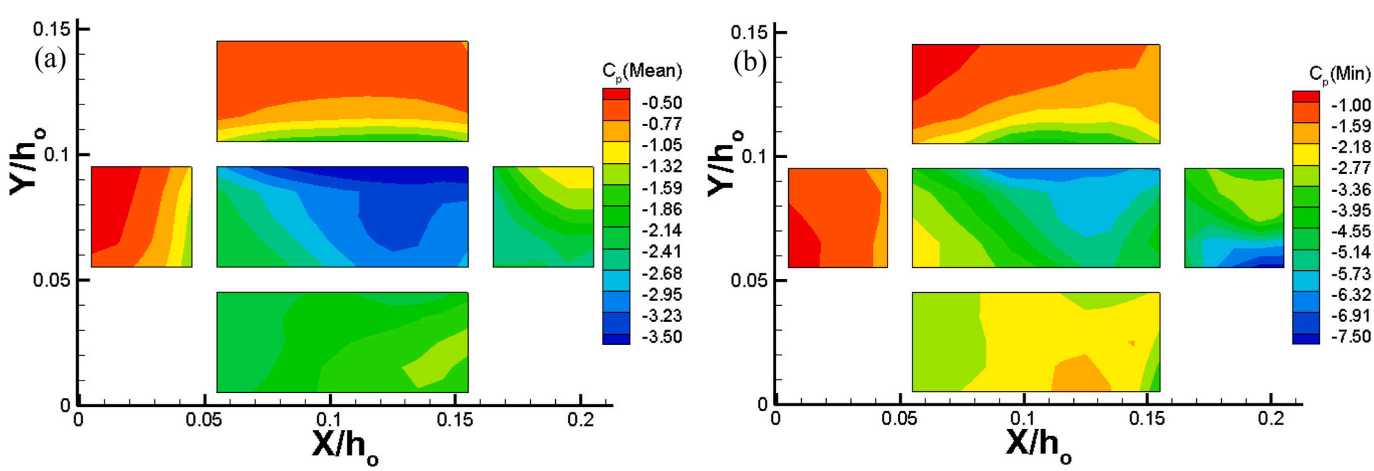

Fig. 15. Pressure contour plot on the faces of the building due to a tornado-like vortex with swirl ratio (S) = 0.15 (before touchdown) when building is located at the center of CFD tornado simulator (a) Mean C_p plot (b) Minimum C_p plot.

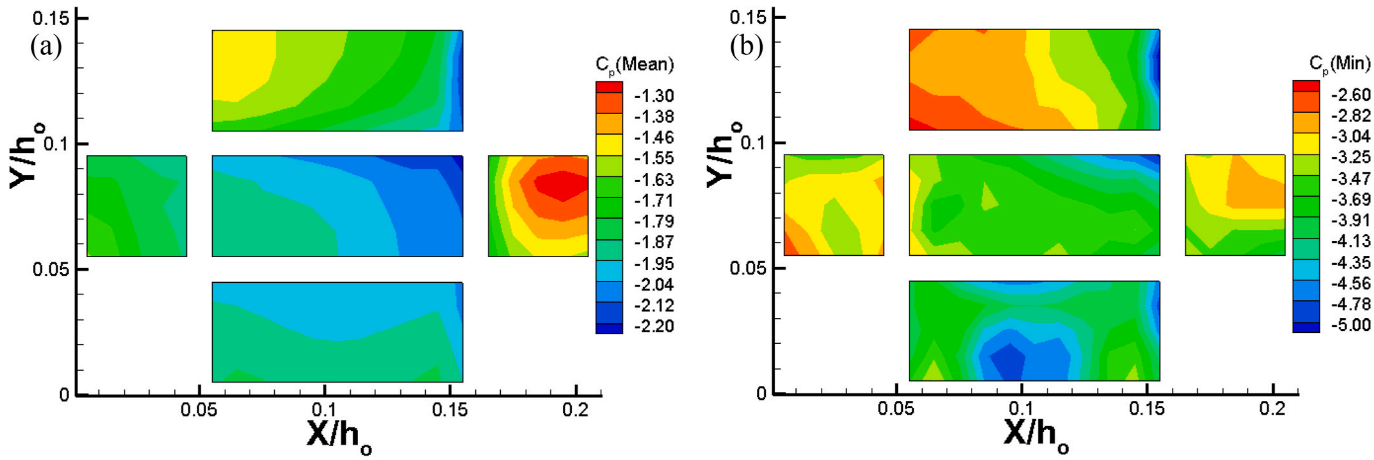

Fig. 16. Pressure contour plot on the faces of the building due to a tornado-like vortex with swirl ratio (S) = 0.36 (during touchdown) when building is located at the center of CFD tornado simulator (a) Mean C_p plot (b) Minimum C_p plot.

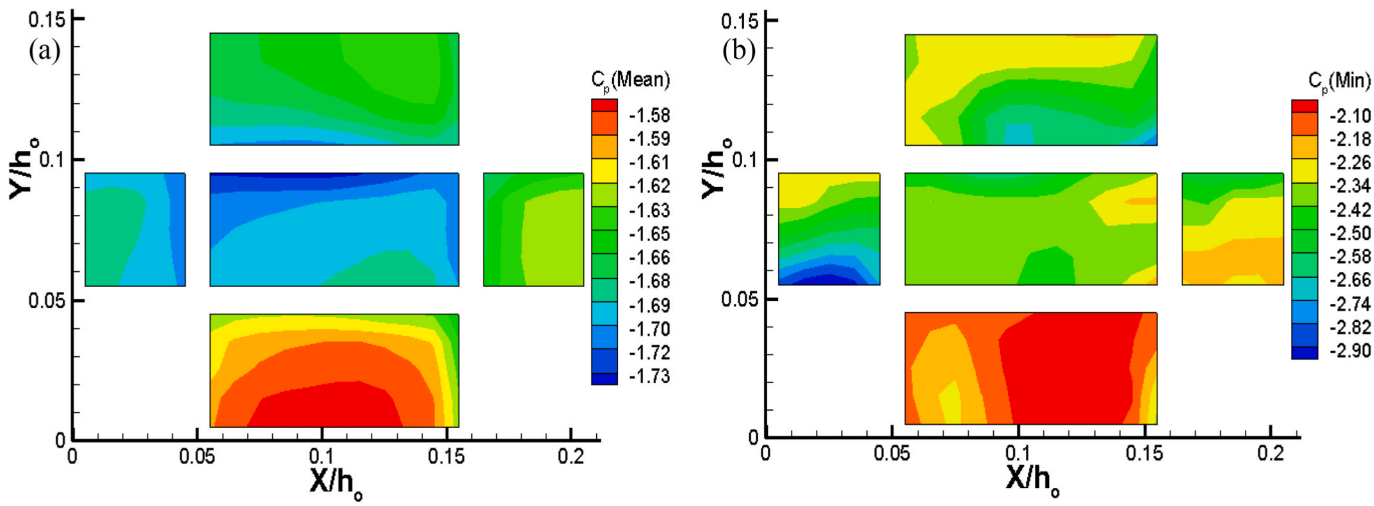

Fig. 17. Pressure contour plot on the faces of the building due to a tornado-like vortex with swirl ratio (S) = 0.83 (post-touched vortex) when building is located at the center of CFD tornado simulator (a) Mean C_p plot (b) Minimum C_p plot.

also demonstrated.

In Fig. 15, the mean and the minimum pressure coefficient (C_p) contour plot due to the interaction of a single-celled tornado-like vortex (S = 0.15) with building is included. From the collected datasets, it is observed that a stationary tornado-like vortex with low swirl ratio can produce drastic loading conditions on a building with a minimum pressure coefficient value as low as −7.5.

Similarly, the mean and the minimum pressure coefficient (C_p) contour plot due to the interaction of a touched-down tornado-like vortex (S = 0.36) with building is included in Fig. 16. From Figs. 15 and 16, it can be observed that the minimum pressure coefficient on the faces of building goes on decreasing with increasing swirl ratios, i.e. minimum $C_p = -7.5$ for S = 0.15 whereas minimum $C_p = -5.0$ for S = 0.36. Similar trend is observed in case of mean pressure coefficient as well in that the minimum mean pressure coefficient drops from $C_p = -3.5$ for S = 0.15 to $C_p = -2.2$ for S = 0.36. Also, the range of both the mean and the minimum pressure coefficient is observed to be decreasing when the swirl ratio of tornado-like vortex is increased from S = 0.15 to S = 0.36.

The mean and the minimum pressure coefficient (C_p) contour plot due to the interaction of a post touched-down vortex (S = 0.83) with building is included in Fig. 17. From Figs. 16 and 17, it can be again observed that the minimum pressure coefficient on the building decreases further to $C_p = -2.90$ when the swirl ratio of vortex increases from S = 0.36 to S = 0.83 and similar trend follows for the mean pressure coefficient as well. Also, the range of both the mean and the minimum pressure coefficient decreases further for S = 0.83 as compared to S = 0.36.

This observation indicates that when the swirl ratio of a stationary tornado-like vortex increases or when the tornado-like vortex gradually transitions from a single-celled vortex to a touched-down or a post-touched down vortex, the effect of drop in static pressure influencing the loading conditions on a building is also gradually reduced. As the swirl ratio of tornado-like vortex increases, the tangential velocity component becomes stronger. Thus, it seems probable that the interaction of tornado-like vortices at high swirl ratio is more dominated by aerodynamic forces that involves separation of detached suction vortices, which then exhibit circular motion around the building rather than the static pressure deficit (Refer Figs. 19–20). Furthermore, the range of pressure coefficient (C_p) is also found to be decreasing when the swirl ratio of tornado-like vortex goes on increasing and this holds true for both the mean and the minimum pressure coefficients. It has been commonly observed that a tornado-like vortex before touchdown bears a slender filament like structure (Rotunno, 2013) with large pressure drops at the center of vortex. Whereas the core of tornado-like vortex becomes larger with increasing value of swirl ratio and the static pressure deficit in the core of tornado-like vortex also becomes lower

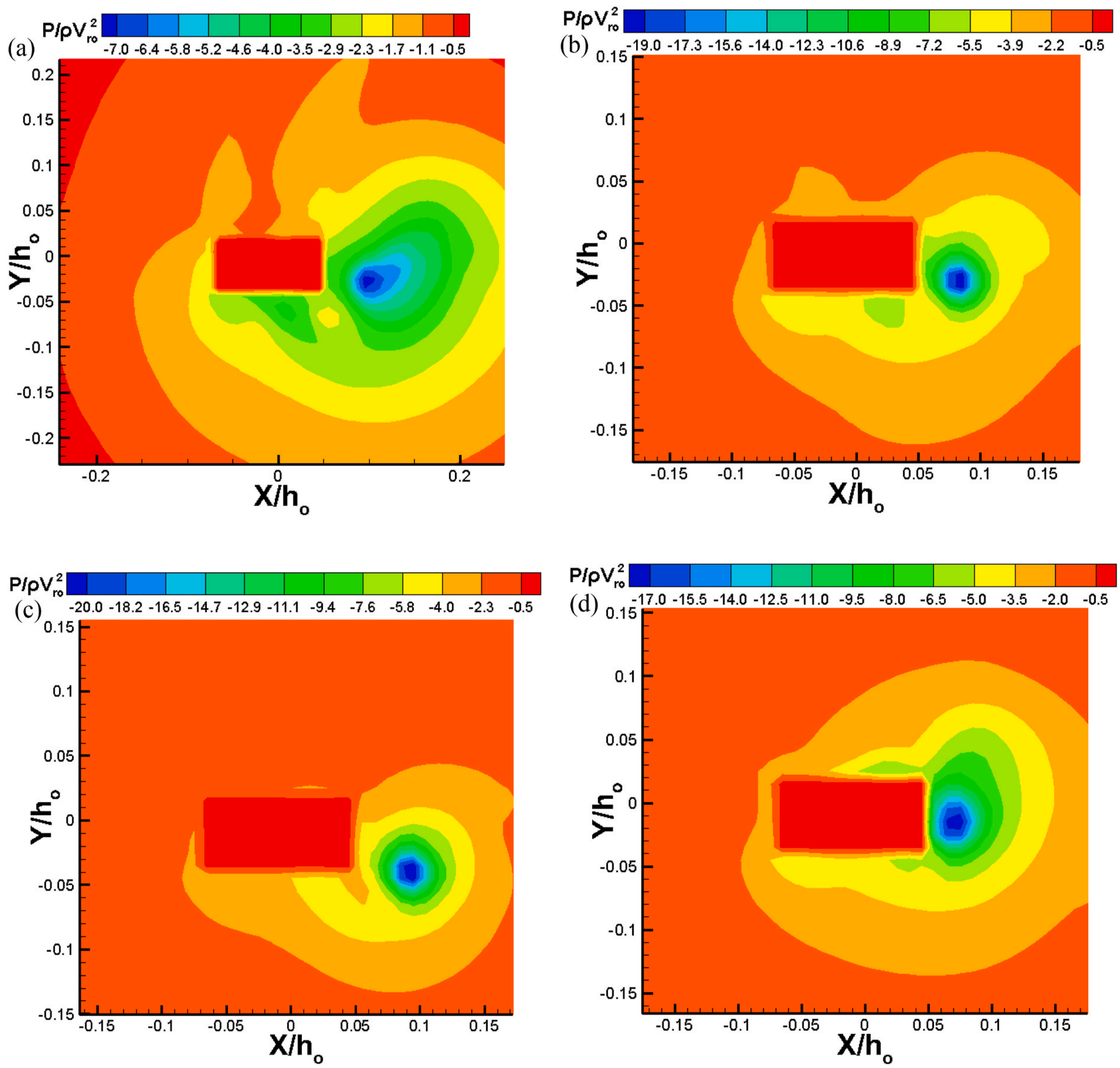

Fig. 18. Suction vortex attached on the eastward face of building for swirl ratio (S) = 0.15 and building located at the center of CFD tornado simulator at 4 different time steps (a) t* = 19.61 (b) t* = 23.47 (c) t* = 25.15 and (d) t* = 29.00.

compared to a single-celled vortex (Tang et al. (2018a, b), Verma and Selvam, 2020). Based on this observation, it can be inferred that a tornado-like vortex interacting with building at higher swirl ratios engulfs a building completely within a larger core radius. However, due to lower drop in static pressure deficit compared to a single-celled vortex as well as lower pressure gradient at the core of vortex, the range of pressure coefficient (C_p) goes on decreasing for larger swirl ratio cases.

In addition, it is observed that the low pressure suction vortex remains attached to the eastward face of the building consistently over different time steps for the lower swirl ratio case (S = 0.15) as shown in Fig. 18. The low pressure suction vortex which remains attached to the building might be the probable cause for a very low value of minimum pressure coefficient ($C_p = -7.5$) in Fig. 15 for S = 0.15. However, in case of a touched-down tornado vortex (with S = 0.36), it has been observed that the low pressure suction vortex gets detached from the face of building and then exhibits a circular motion around the building. As the suction vortices detach from the face of building and exhibit a circular motion, the vortex dynamics changes and thus the aerodynamic forces dominate over the forces resulting from static pressure drop. Consequently, the pressure coefficient as well as the range of pressure coefficient on the faces of building decreases.

The flow field of tornado-like vortex around the building for S = 0.15 starting from non-dimensional time of t* = 19.61 units to t* = 29.00 units is shown in Fig. 18, which demonstrates that the low pressure suction vortex remains attached to the eastward face of building in each of the time steps. Whereas for a tornado-like vortex during touchdown (S = 0.36) and after touchdown (S = 0.83), the low pressure suction vortex detaches from the face of building and exhibits a circular motion around the building as shown in Figs. 19 and 20. The unsteady detached suction vortices in the periphery of building seems somewhat comparable to Von Karman vortex street observed in straight line wind flows. In a straight line wind flow around a solid object, the vortices detach from the solid object and are carried away in streamwise direction of flow beyond a certain critical Reynolds number. However, in tornado-like flow, the detached vortices begin to exhibit circular motion around the solid object (building) under the influence of tangential and radial velocity components. The detached suction vortices in the periphery of building is unsteady in nature and could be another contributing factor for wind load on buildings during tornadic events as these vortices possess momentum due to its circular motion. When these

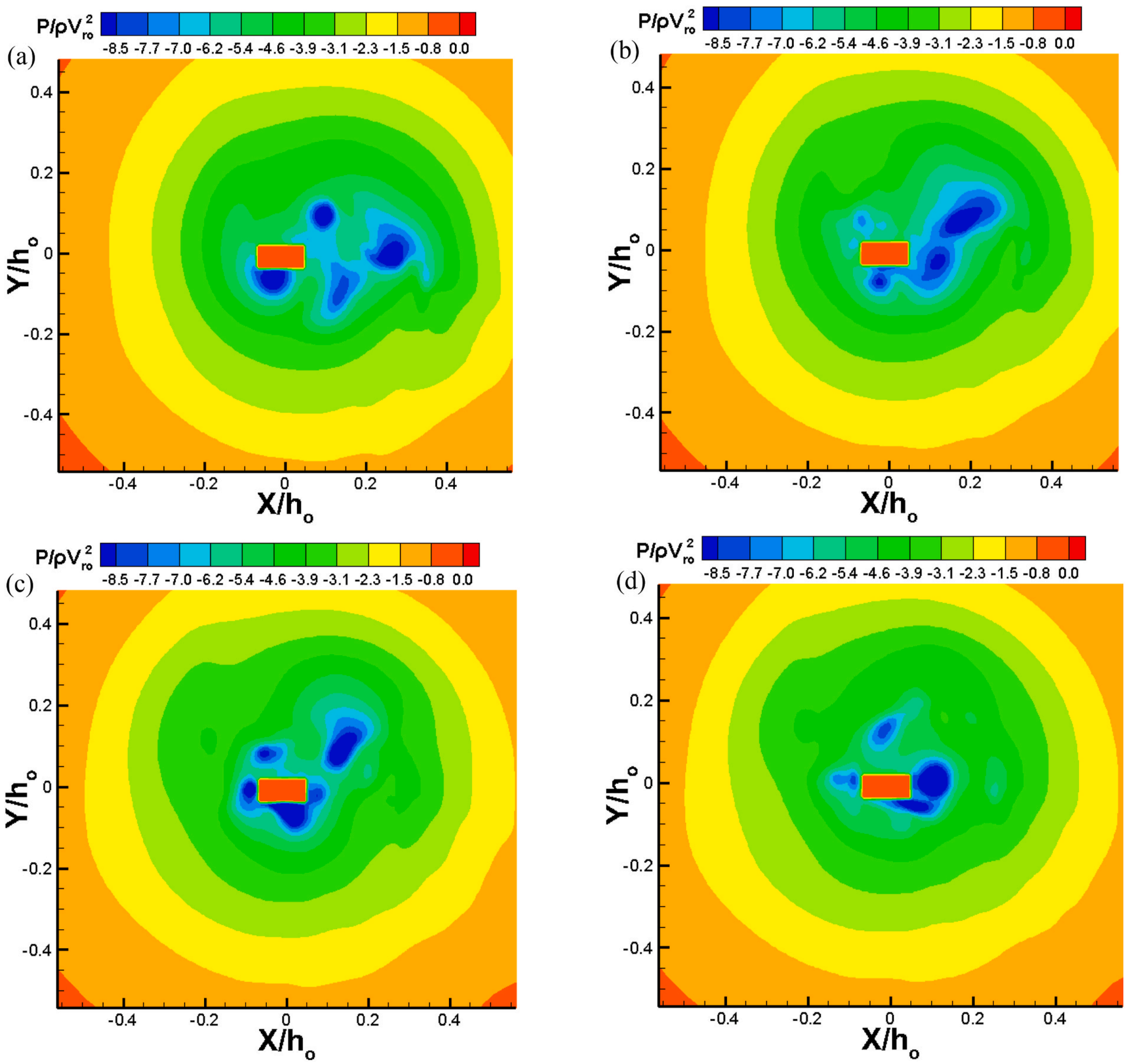

Fig. 19. Detached suction vortices in the periphery of building for swirl ratio (S) = 0.36 and building located at the center of CFD tornado simulator at 4 different time steps (a) t* = 17.96 (b) t* = 22.95 (c) t* = 25.82 and (d) t* = 28.12.

vortices transfer their momentum to stationary buildings during the impact then, it can produce impact loading on the buildings. However, in this relatively simplistic model, such dynamic effects have not been considered, so, the mean as well as the minimum pressure coefficients may be much higher for the single-celled tornado-like vortex (S = 0.15) than the touched-down (S = 0.36) or double-celled vortex (S = 0.83). Hence, considering the induced wind loads on building due to static pressure drop, tornado-like vortex before touchdown seems to be more devastating than a vortex during and beyond touchdown. Nevertheless, the impact loading due to exchange of momentum between the detached suction vortices around the building and the stationary building could be another important factor contributing to the induced loads as well as the disintegration of building envelope.

In general, the induced negative pressures on the building is reduced for the case when the building is placed at the location of core radius as compared to the center of tornado-like vortex. This is due to the direct impact of tangential velocity component on the building resulting in positive pressures. Thus, the magnitude of negative pressures is most likely to decrease for the case when building is placed at core radius rather than at the center of tornado-like vortex. However, it is observed from the collected datasets in this study that suction vortices formed in the periphery of building remains attached to the building for a low swirl ratio case (S = 0.15) as shown in Fig. 24. The suction vortices that remain attached on the building is most likely the reason for low mean and minimum pressure coefficient ($C_p = -5.0$ for mean and $C_p = -7.0$ for minimum respectively) on the building in Fig. 21 below. However, in case of a touched-down (S = 0.36) and post-touched-down vortex (S = 0.83), the low pressure suction vortices is observed to detach from the face of building and then exhibit circular motion around the building. The detached suction vortices revolve around the building with different radii; the radius for higher swirl ratio (S = 0.83) is greater than that for S = 0.36. Despite the anticipated direct impact of tangential velocity component reducing the negative pressures on the building, it is observed that the suction vortices that detach from the building during the circular motion around the building could impact the building as well as get attached to the building momentarily. The pressure drop in these suction vortices is a lot higher than that of the surrounding core region of vortex. Thus, it seems to be the reason for higher magnitude of negative pressures on the building even when the building is placed at core radius location. The mean and the minimum pressure coefficient contour plots when the bulding is placed at core radius of tornado-like vortex for different swirl ratios (S = 0.15, 0.36 and 0.83) are included

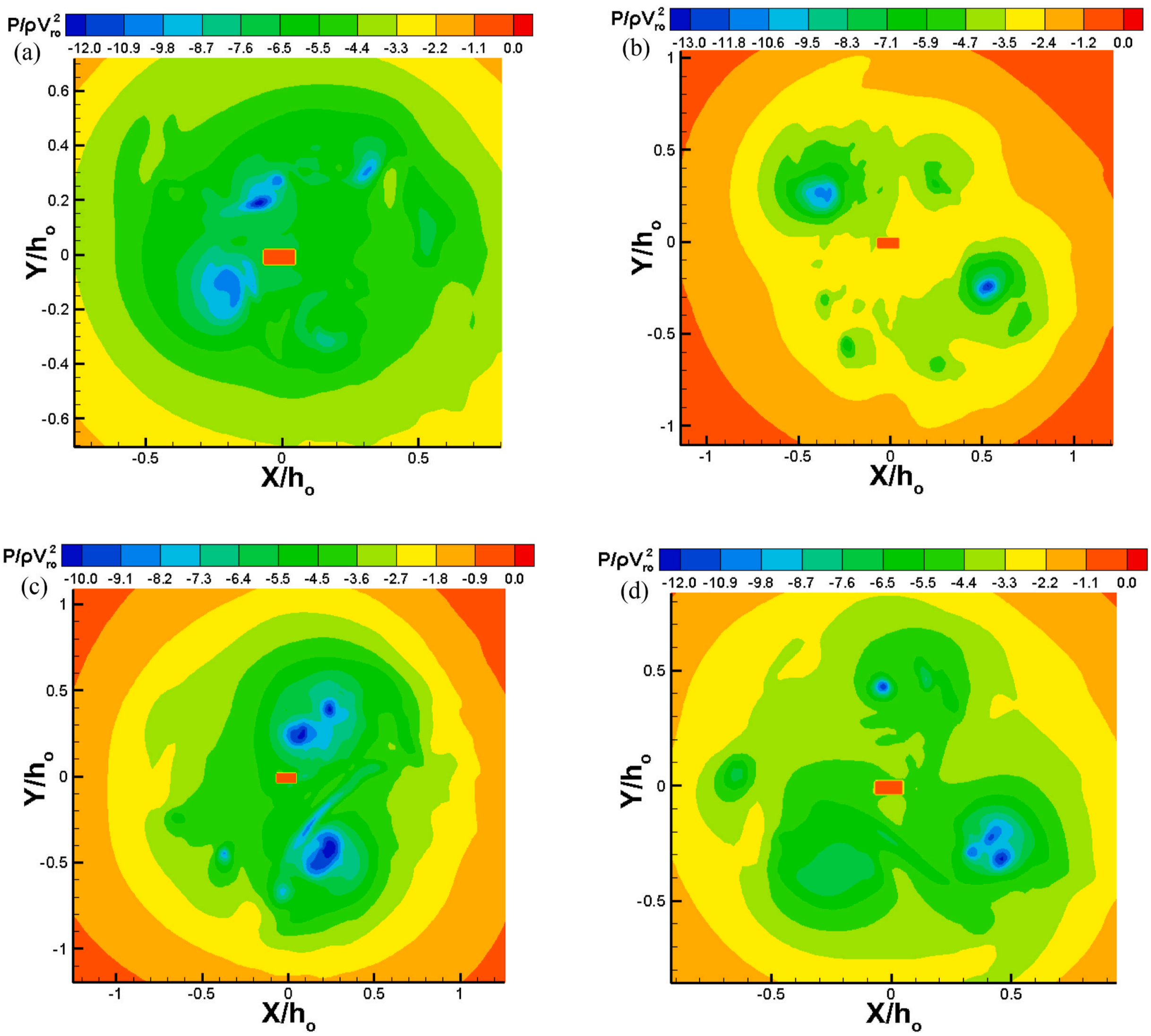

Fig. 20. Detached suction vortices in the periphery of building for swirl ratio (S) = 0.83 and building located at the center of CFD tornado simulator at 4 different time steps (a) t* = 17.96 (b) t* = 22.95 (c) t* = 25.82 and (d) t* = 28.12.

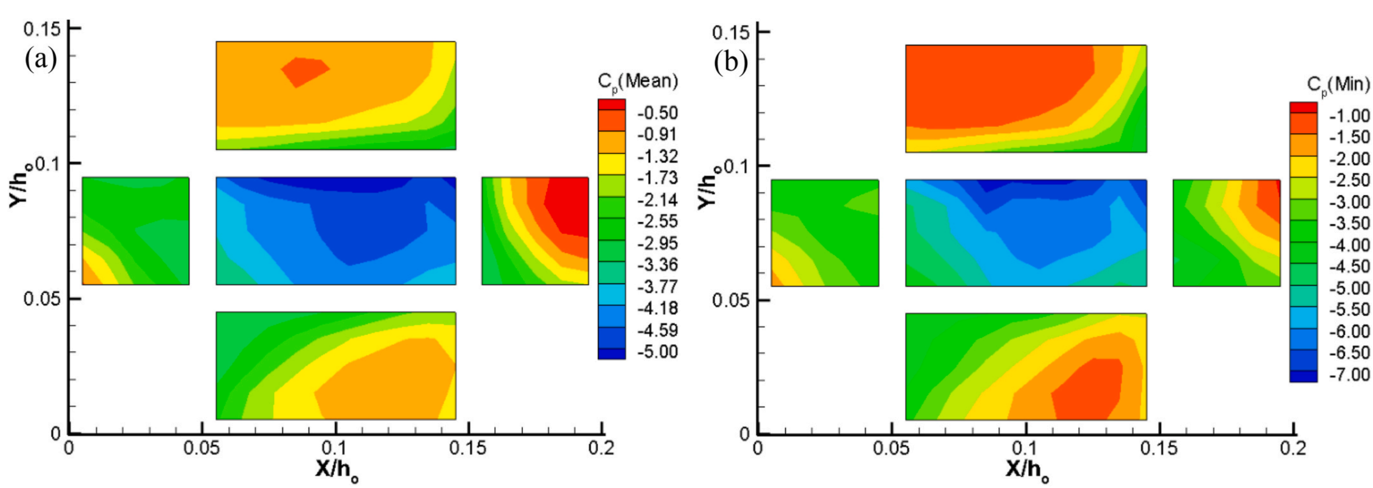

Fig. 21. Pressure contour plot on the faces of the building due to a tornado-like vortex with swirl ratio (S) = 0.15 (before touchdown) when building is located at core radius of tornado-like vortex (a) Mean C_p plot (b) Minimum C_p plot.

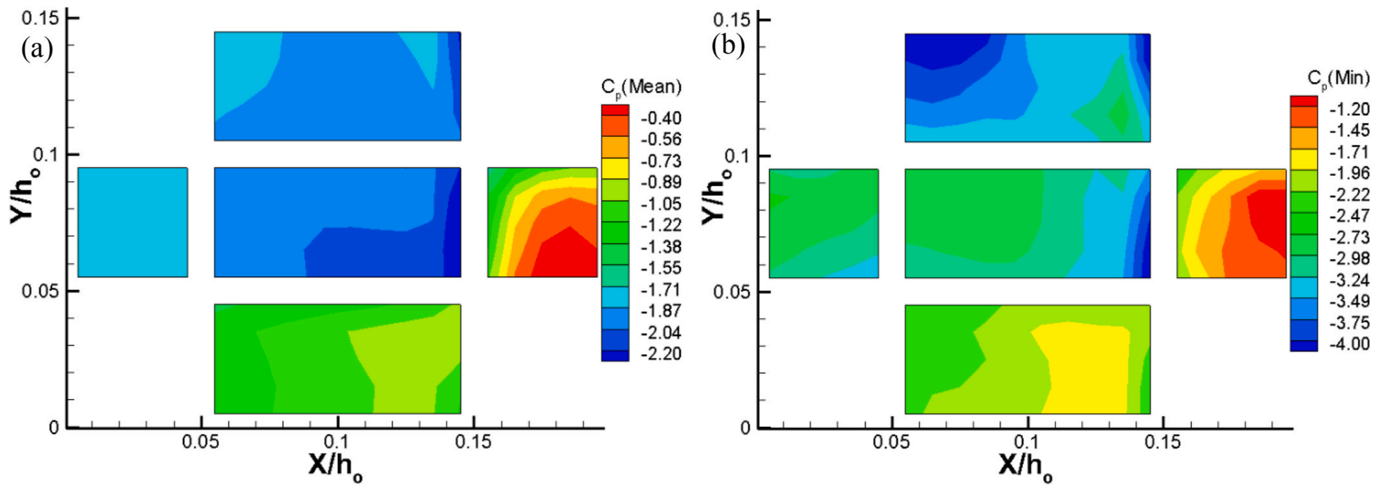

Fig. 22. Pressure contour plot on the faces of the building due to a tornado-like vortex with swirl ratio (S) = 0.36 (during touchdown) when building is located at core radius of tornado-like vortex (a) Mean C_p plot (b) Minimum C_p plot.

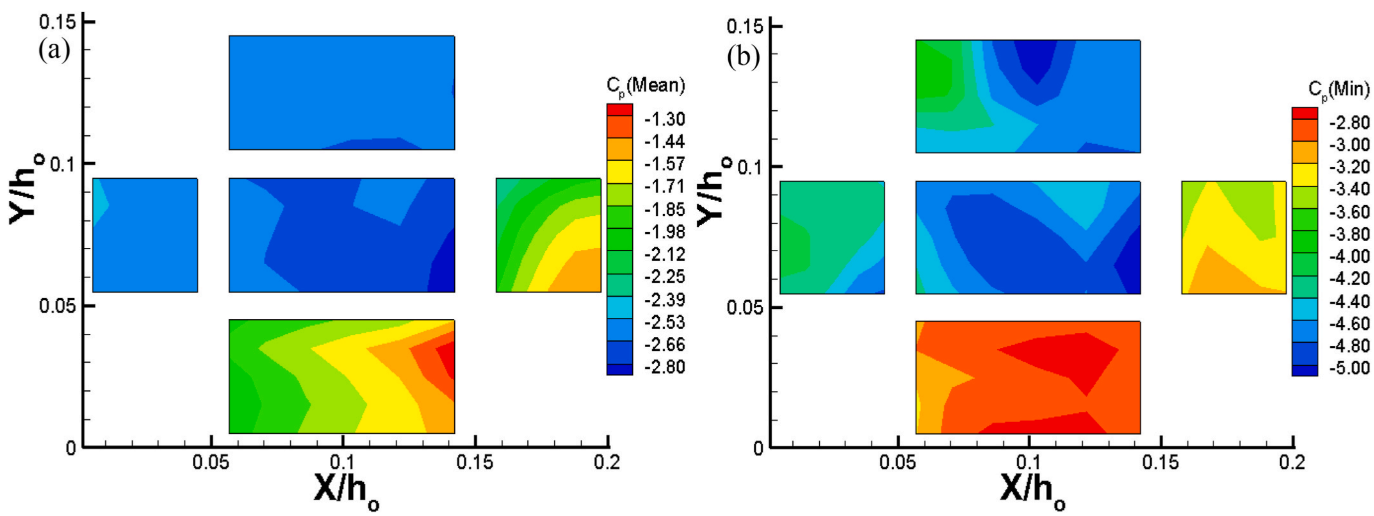

Fig. 23. Pressure contour plot on the faces of the building due to a tornado-like vortex with swirl ratio (S) = 0.83 (post-touchdown vortex) when building is located at core radius of tornado-like vortex (a) Mean C_p plot (b) Minimum C_p plot.

in Figs. 21–23. Similarly, the suction vortices that remain attached to the building for S = 0.15 and the detached suction vortices revolving around the bulding for S = 0.36 and S = 0.83 are included in Figs. 24–26.

Hence, based on the datasets obtained from the CFD model, it is concluded that the interaction of wind field of a stationary tornado-like vortex at low swirl ratio (or a single-celled tornado vortex) produces the severest suction pressure (minimum C_p as low as −7.71) and thus creates the most adverse loading conditions on a building. In case of a touched-down tornado-like vortex or a vortex beyond touchdown, a number of small suction vortices are observed around the building and the pressure drop in such suction vortices is much higher compared to the core of tornado-like vortex. Due to the sharp drop in pressure within the suction vortices, it seems that the suction pressure on the faces of building remains high even when the building is placed at core radius. Previous work by Razavi and Sarkar (2018) and Li et al. (2020) had reported similar conclusion that a single-celled vortex creates the most unfavorable loading conditions on a building. However, the magnitude of C_p reported in earlier studies is lower than the values reported in this work. This could be due to different geometrical configuration and flow generation mechanism in different simulators, different grid resolution and/or differences in pressure boundary condition. The mean and the minimum C_p obtained on the faces of building due to the interaction of different swirl ratio vortex is reported in Table 5.

For mean pressures on building, the core radius of vortex seems more critical as compared to the center of vortex since the minimum of mean C_p occurs at the location of core radius for all the three flow structures of vortex (S = 0.15, 0.36, 0.83) in Table- 5. For the vortex before touchdown (S = 0.15), mean C_p varies in the range of −3.885 to −0.363 when the building is placed at the center of vortex whereas for the same flow structure, the mean C_p varies in the range of −5.422 to −0.204 when the building is placed at the location of core radius. So, it might be appropriate to design the main wind force resisting system of the building considering the mean C_p obtained at the location of core radius. In the future, more exhaustive case studies can be done to verify this conclusion. On the other hand, the minimum pressure coefficient on the building placed at the center of vortex (−7.709) is slightly higher than the minimum C_p at the location of core radius (−7.214). However, an observation can be made that the core radius of a single-celled vortex is as critical as the center considering the forces on building due to static pressure deficit. Both the minimum pressure coefficient and the range of minimum C_p on the building goes on decreasing with increasing value of swirl ratios. Thus, for component & cladding, the minimum pressure coefficients due to a single-celled vortex might be appropriate for design purposes.

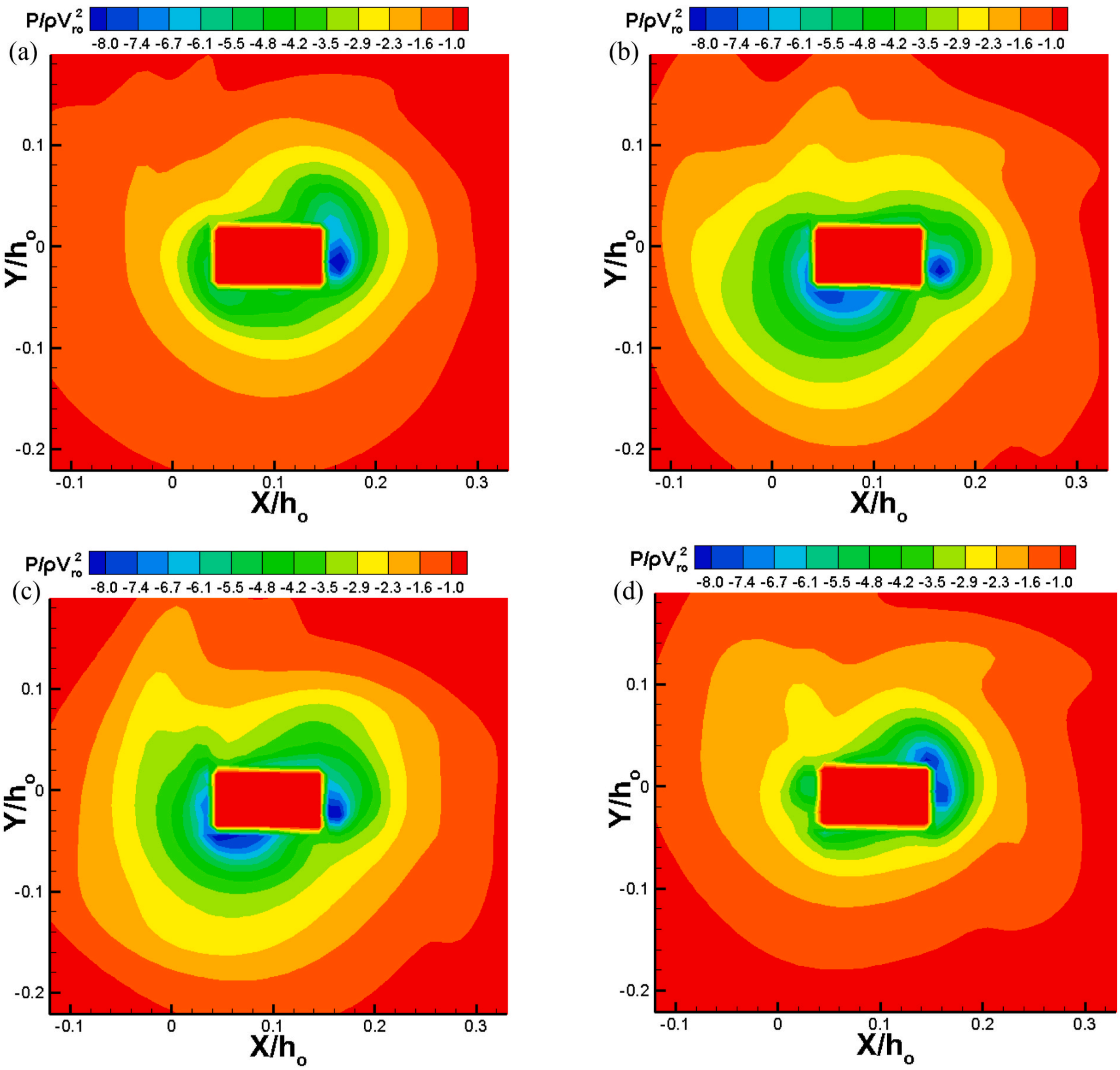

Fig. 24. Suction vortex attached on the periphery of building when the building is placed at core radius for swirl ratio (S) = 0.15 at 4 different time steps (a) t* = 20.17 (b) t* = 24.13 (c) t* = 26.90 and (d) t* = 29.92.

5. Conclusion

In previous CFD studies, the pressure coefficients obtained on the building model lacked a one-to-one comparison with experimental datasets. So, in this work, the pressure coefficients are computed on a building model having the same dimensions as the one used in VorTECH simulator and using the same swirl ratio (S = 0.83) vortex as the VorTECH simulator. The pressure coefficients on the building obtained from CFD model compare reasonably well with experimental measurements from the VorTECH simulator at TTU. The major conclusions from this work as summarized below:

- The mean C_p ranges from −1.58 to −1.73 on the building VCBM1 for the CFD model whereas for the TTU experiment, the corresponding values range from −1.49 to −1.65. So, the pressure coefficients predicted by the CFD model shows deviation from the experimental datasets by about 5.4% on average. From the comparison of mean C_p profile along the centerline of the building between the CFD model and TTU experiment, the NRMSE is obtained at about 9.11% for the case when building is located at center of vortex. Based on a reasonable agreement (with percentage error <10%) in the values of C_p predicted by the CFD model, the model is said to be validated with TTU experiment.
- For the building VCBM1 (dimensions $0.10h_o$ x $0.05h_o$ x $0.05h_o$), the mean C_p ranges from −1.25 to −0.96 whereas for building2 (dimensions $0.10h_o$ x $0.10h_o$ x $0.10h_o$), the mean C_p ranges from −2.30 to −2.05 when the building is at the center of vortex. Similarly, the minimum C_p varies in the range from −3.00 to −2.03 for VCBM1 and from −7.33 to −3.57 for building2 when the building is at the center of vortex. The values of C_p for building2 are almost twice that of VCBM1. So, the induced pressures on the building can differ by about 100% when the building of different sizes/scale are used in a tornado simulator with all the relevant flow conditions remaining constant. Hence, it seems critically important to establish a reference or a benchmark model for size (or scale) of building for future studies on interaction of wind field of tornado-like vortex with buildings.
- The mean pressure coefficients on the building placed at the center of vortex varies in the range of −0.363 to −3.885, −1.246 to −2.247 and −1.571 to −1.736 for S = 0.15, S = 0.36 and S = 0.83 respectively. Similarly, the mean pressure coefficients on the building

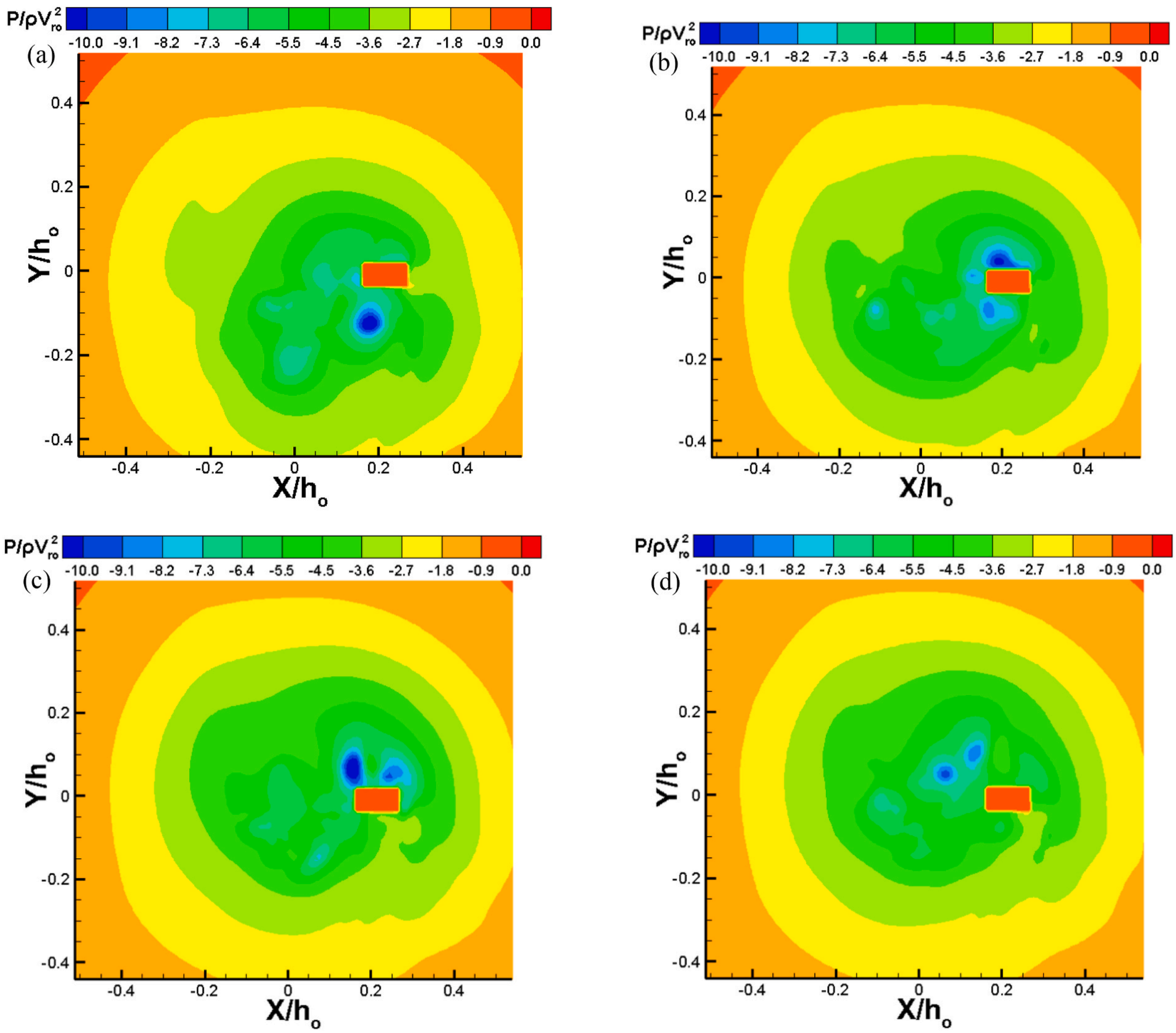

Fig. 25. Detached suction vortices around the building when the building is placed at core radius for swirl ratio (S) = 0.36 at 4 different time steps (a) t* = 24.93 (b) t* = 25.14 (c) t* = 25.63 and (d) t* = 25.73.

placed at core radius of vortex varies in the range of −0.204 to −5.422, −0.266 to −2.426 and −1.201 to −2.889 for S = 0.15, S = 0.36 and S = 0.83 respectively. For mean C_p, the core radius of vortex seems more critical as compared to the center since the minimum of mean C_p occurs at the location of core radius for all the flow structures of vortex (S = 0.15, 0.36, 0.83) considered in this study. So, it might be more appropriate to design the main wind force resisting system of the building using the mean C_p obtained at the location of core radius.

- The minimum pressure coefficient on the building placed at the center of vortex varies in the range of −0.623 to −7.709, −2.509 to −5.162 and −2.301 to −3.000 for S = 0.15, S = 0.36 and S = 0.83 respectively. Similarly, the minimum pressure coefficient on the building placed at core radius of vortex varies in the range of −0.876 to −7.214, −0.980 to −4.247 and −2.652 to −5.223 for S = 0.15, S = 0.36 and S = 0.83 respectively. The minimum pressure coefficient on the building placed at the center of vortex (−7.709) is slightly higher than the minimum C_p at the location of core radius (−7.214). However, it can be said that the core radius of a single-celled vortex is as critical as the center considering the forces on building due to static pressure deficit. For component & cladding, the minimum pressure coefficient due to a single-celled vortex when the building is at the center might be appropriate for design purposes. In the future, more exhaustive research should be carried out to verify these observations for developing wind load provisions.
- An interesting phenomenon of the interaction of turbulent structures (suction vortices) with the building due to varying flow structure of tornado-like vortex is also reported in this work, which is not available in previous studies. It is observed that a suction vortex is formed in the vicinity of building in case of a single-celled vortex, which remains attached to the surface of building consistently over several time-steps. Whereas in case of a touched-down and post-touched-down vortex, **several** small suction vortices are observed to have formed around a building which detach from the face of the building and then exhibit a circular motion in the periphery of building model. A better understanding of the interaction of these suction vortices with the building could help to develop a better understanding of the aerodynamic interaction of tornado-like vortices with building model. Further work will be carried out in that direction in the future to understand the cause and effect of the turbulent structures (suction vortices) on the induced wind loads on buildings.

CRediT authorship contribution statement

Sumit Verma: Methodology, Investigation, Data curation, Formal analysis, Writing – original draft, Validation, Visualization. **R. Panneer**

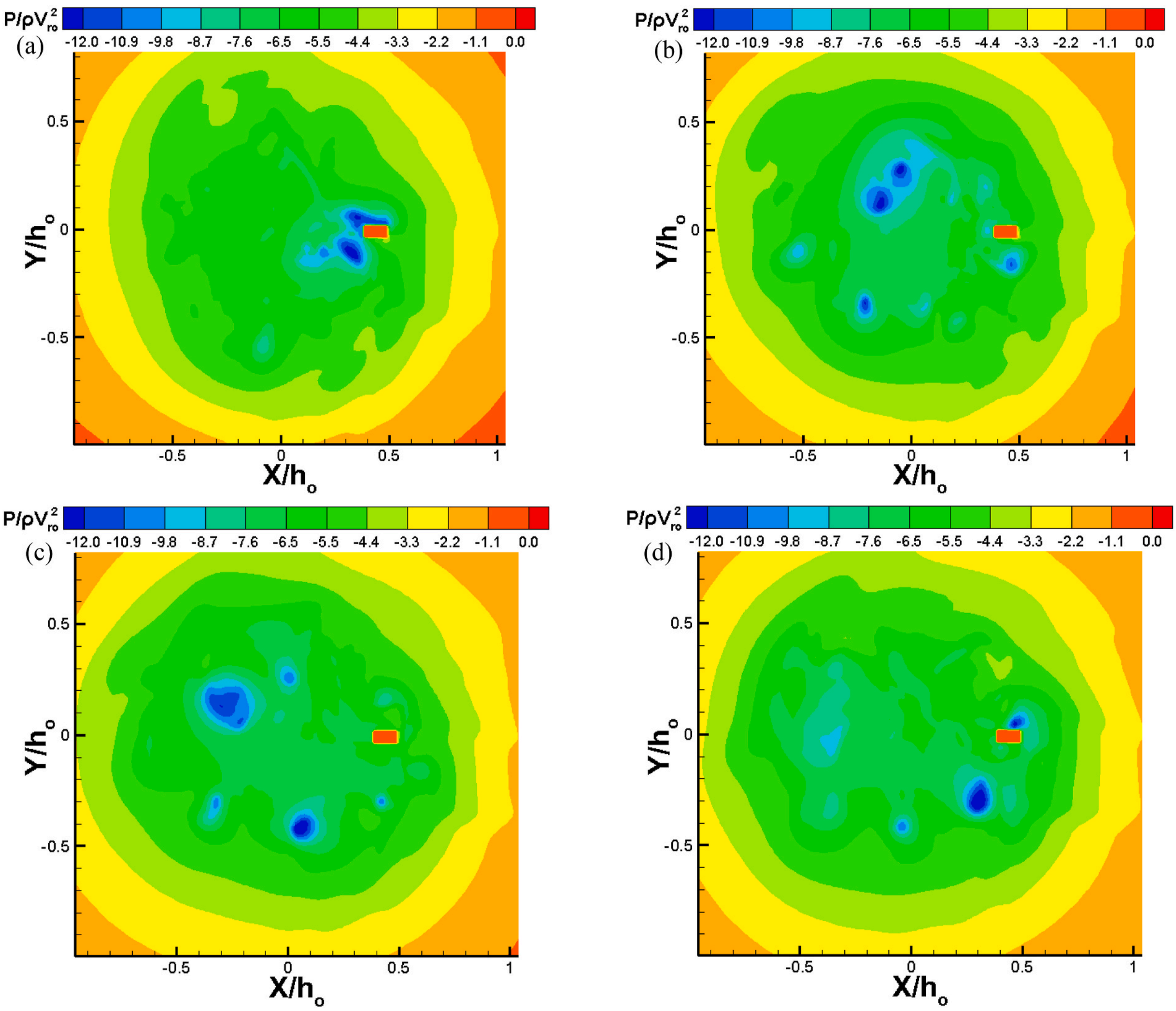

Fig. 26. Detached suction vortices around the building when the building is placed at core radius for swirl ratio (S) = 0.83 at 4 different time steps (a) t* = 20.27 (b) t* = 20.80 (c) t* = 20.97 and (d) t* = 21.16.

Table 5
Range of mean and the minimum C_p on the faces of building due to different swirl ratios of tornado-like vortices when building placed is placed at the center of simulator and location of core radius.

S.N.	Swirl ratio	$r/r_c = 0$				$r/r_c = 1$			
		Mean C_p		Minimum C_p		Mean C_p		Minimum C_p	
		Min.	Max.	Min.	Max.	Min.	Max.	Min.	Max.
1	0.15	−3.885	−0.363	−7.709	−0.623	−5.422	−0.204	−7.214	−0.876
2	0.36	−2.247	−1.246	−5.162	−2.509	−2.426	−0.266	−4.247	−0.98
3	0.83	−1.736	−1.571	−3.000	−2.301	−2.889	−1.201	−5.223	−2.652

Selvam: Conceptualization, Writing – review & editing, Software, Supervision, Project administration, Funding acquisition. **Zhuo Tang:** Experimental testing, Resources, Writing – review & editing. **Delong Zuo:** Experimental datasets, Resources, Writing – review & editing.

Declaration of competing interest

The authors declare the following financial interests/personal relationships which may be considered as potential competing interests: R. Panneer Selvam reports financial support was provided by National Science Foundation.

Data availability

Data will be made available on request.

Acknowledgments

The authors acknowledge the support received from National Science Foundation (NSF) under the award number CMMI-1762999.

References

Alexander, C.R., Wurman, J., 2005. The 30 may 1998 spencer, south Dakota, storm. Part I: the structural evolution and environment of the tornadoes. Mon. Weather Rev. 133, 72–97.

Alipour, A., Sarkar, P., Dikshit, S., Razavi, A., Jafari, M., 2020. Analytical approach to characterize tornado-induced loads on lattice structures. J. Struct. Eng. 146, 04020108. Article.

Alrasheedi, N.H., Selvam, R.P., 2011. Tornado Forces on Different Building Sizes Using Computer Modeling, *2011 ECTC Proceedings, ASME Early Career Technical Conference*. Hosted by ASME District E and University of Arkansas, Fayetteville. March 31-April 02.

Bluestein, H.B., Pazmany, A.L., 2000. Observations of tornadoes and other convective phenomena with a mobile, 3-mm wavelength, Doppler radar: the spring 1999 field experiment. Bull. Am. Meteorol. Soc. 81, 2939–2952.

Cengel, Y.A., Cimbala, J.M., 2014. Fluid Mechanics: Fundamentals and Applications, third ed. McGraw Hill, New York.

Changnon, S.A., 2009. Tornado losses in the United States. Nat. Hazards Rev. 10 (4), 145–150. https://doi.org/10.1061/(asce)1527-6988(2009)10:4(145).

Gairola, A., Bitsuamlak, G.T., 2018. On the application of generic numerical tornado model to evaluate tornadic wind loads on structures. In: *CSCE Conference: Building Tomorrow's Society*, Fredericton. Canada, June 13-16, 2018.

Gairola, A., Bitsuamlak, G., 2019. Numerical tornado modeling for common interpretation of experimental simulators. J. Wind Eng. Ind. Aerod. 186, 32–48.

Gillmeier, S., 2019. An Investigation Concerning the Simulation of Tornado-like Vortices. Ph.D. Dissertation, University of Birmingham, Birmingham, U.K.

Haan, F.L., Sarkar, P., Gallus, W.A., 2008. Design, construction and performance of a large tornado simulator for wind engineering applications. Eng. Struct. 30, 1146–1159.

Haan Jr., F.L., Balaramudu, V.K., Sarkar, P.P., 2010. Tornado-induced wind loads on a low-rise building. J. Struct. Eng. 136, 106–116.

Hangan, H., 2014. The Wind Engineering Energy and Environment (WindEEE) Dome at Western University, 39. Wind Engineers, JAWE, Canada.

Harlow, F.H., Stein, L.R., 1974. Structural analysis of tornado-like vortices. J. Atmos. Sci. 31, 2081–2098.

Hirt, C.W., Cook, J.L., 1972. The calculation of three-dimensional flows around structures and over rough terrain. J. Comput. Phys. 10, 324–340.

Hu, H., Yang, Z., Sarkar, P., et al., 2011. Characterization of the wind loads and flow fields around a gable-roof building model in tornado-like winds. Exp. Fluid 51, 835.

Ishihara, T., Oh, S., Tokuyama, Y., 2011. Numerical study on flow fields of tornado-like vortices using the LES turbulence model. J. Wind Eng. Ind. Aerod. 99, 239–248.

Kashefizadeh, M.H., Verma, S., Selvam, R.P., 2019. Computer modelling of close-to-ground tornado wind-fields for different tornado widths. J. Wind Eng. Ind. Aerod. 191, 32–40.

Kikitsu, H., Okuda, Y., 2016. Tornado-induced wind load model on a building considering relative size of building and tornado-like vortex. In: *Proc., 6th U.S.-Japan Workshop On Wind Engineering*. Iowa State Univ, Yokohama, Kanagawa: Yokohama National Univ. and Ames, IA, pp. 12–14.

Kosiba, K.A., Wurman, J., 2010. The three-dimensional axisymmetric wind field structure of the Spencer, South Dakota, 1998, tornado. J. Atmos. Sci. 67, 3074–3083.

Kosiba, K.A., Wurman, J., 2013. The three-dimensional structure and evolution of a tornado boundary layer. Weather Forecast. 28, 1552–1561.

Kuai, L., Haan, F.L., Gallus, W.A., Sarkar, P.P., 2008. CFD simulations of the flow field of a laboratory-simulated tornado for parameter sensitivity studies and comparison with field measurements. Wind Struct. 11, 75–96.

Lewellen, W.S., Lewellen, D.C., Sykes, R.I., 1997. Large-eddy simulation of a tornado's interaction with the surface. J. Atmos. Sci. 54, 581–605.

Lewellen, D.C., Lewellen, W.S., 2007. Near-surface intensification of tornado vortices. J. Atmos. Sci. 64, 2176–2194.

Li, T., Yan, G., Yuan, F., Chen, G., 2019. Dynamic structural responses of long-span dome structures induced by tornadoes. J. Wind Eng. Ind. Aerod. 190, 293–308.

Li, T., Yan, G., Feng, R., Mao, X., 2020. Investigation of the flow structure of single- and dual-celled tornadoes and their wind effects on a dome structure. Eng. Struct. 209, 109999.

Liu, Z., Ishihara, T., 2015. A study of tornado induced mean aerodynamic forces on a gable-roofed building by the large eddy simulations. J. Wind Eng. Ind. Aerod. 146, 39–50.

Mishra, A.R., James, D.L., Letchford, C.W., 2008. Physical simulation of a single-celled tornado-like vortex, Part B: wind loading on a cubical model. J. Wind Eng. Ind. Aerod. 96, 1258–1273.

Molloy, S.L., Mihaltcheva, S., 2013. 1.01 - Extreme weather events. In: Roger A. Pielke, *Climate Vulnerability*. Academic Press, pp. 3–16.

Nasir, Z., Bitsuamlak, G.T., Hangan, H., 2014. Computational Modeling of Tornadic Load on a Building, *6th International Symposium On Computational Wind Engineering*. Hamburg, Germany, June 8-12, 2014.

Nasir, Z., Bitsuamlak, G.T., 2016. NDM-557: computational modeling of hill effects on tornado-like vortex. In: CSCE Annual Conference. London Convention Center, London, Ontario, Canada.

Nolan, D.S., Farrell, B.F., 1999. The structure and dynamics of tornado-like vortices. J. Atmos. Sci. 56, 2908–2936.

Razavi, A., Sarkar, P., 2018. Tornado-induced wind loads on a low-rise building: influence of swirl ratio, translation speed and building parameters. Eng. Struct. 167, 1–12.

Refan, M., Hangan, H., 2016. Characterization of tornado-like flow fields in a new model scale wind testing chamber. J. Wind Eng. Ind. Aerodyn. 151, 107–121.

Refan, M., Hangan, H., 2018. Near surface experimental exploration of tornado vortices. J. Wind Eng. Ind. Aerodyn. 175, 120–135.

Rotunno, R., 1979. A study in tornado-like vortex dynamics. J. Atmos. Sci. 36, 140–155.

Rotunno, R., 2013. The fluid dynamics of tornadoes. Annu. Rev. Fluid Mech. 45, 59–84.

Sabareesh, G.R., Matsui, M., Tamura, Y., 2012. Dependence of surface pressures on a cubic building in tornado like flow on building location and ground roughness. J. Wind Eng. Ind. Aerod. 103, 50–59.

Sabareesh, G.R., Matsui, M., Tamura, Y., 2013. Ground roughness effects on internal pressure characteristics for buildings exposed to tornado-like flow. J. Wind Eng. Ind. Aerod. 122, 113–117.

Selvam, R.P., 1997. Finite element modelling of flow around a circular cylinder using LES. J. Wind Eng. Ind. Aerod. 67–68, 129–139.

Selvam, R.P., Millett, P.C., 2003. Computer modeling of tornado forces on buildings. Wind Struct. 6, 209–220.

Selvam, R.P., Millett, P.C., 2005. Large eddy simulation of the tornado-structure interaction to determine structural loadings. Wind Struct. 8, 49–60.

Selvam, R.P., Gorecki, P., 2012. Effect of Tornado Size on Forces on Thin 2D Cylinder. *3rd American Association for Wind Engineering Workshop*, Hyannis, MA, USA, pp. 1–9.

Sengupta, A., Haan, F.L., Sarkar, P.P., Balaramudu, V., 2008. Transient loads on buildings in microburst and tornado winds. J. Wind Eng. Ind. Aerod. 96, 2173–2187.

Tang, Z., Feng, C., Wu, L., et al., 2018 a. Characteristics of tornado-like vortices simulated in a large scale ward type simulator. Boundary-Layer Meteorol. 166, 327–350.

Tang, Z., Zuo, D., James, D., et al., 2018 b. Effects of aspect ratio on laboratory simulation of tornado-like vortices. Wind Struct. 27, 111–121.

Verma, S., Selvam, R.P., 2020. CFD to VorTECH pressure field comparison & roughness effect on flow. J. Struct. Eng. 146, 04020187-1 to 12.

Verma, S., Selvam, R.P., 2021a. Effect of height of the tornado chamber on vortex touchdown. In: Rushi Kumar, B., Sivaraj, R., Prakash, J. (Eds.), Advances in Fluid Dynamics. Lecture Notes in Mechanical Engineering. Springer, Singapore.

Verma, S., Selvam, R.P., 2021b. Differences in flow structures of tornado vortex and efficiency of different tornado chambers. In: 6th AAWE Workshop Organized by Clemson University available from: https://tigerprints.clemson.edu/cgi/viewcontent.cgi?article=1075&context=aawe.

Verma, S., Selvam, R.P., 2021c. CFD model validation with experimental tornado wind field & comparison of wind field in different tornado chambers. Wind Struct. 33, 367–381.

Verma, S., 2022. Validation of CFD Tornado Pressure on Building and Wind Field with TTU Vortex Chamber Measurements. Ph.D. dissertation. University of Arkansas, Fayetteville, USA.

Yang, Z., Sarkar, P., Hu, H., 2011. An experimental study of a high-rise building model in tornado-like winds. J. Fluid Struct. 27, 471–486.

Yousef, M.A., Selvam, P.R., Prakash, J., 2018. A comparison of the forces on dome and prism for straight and tornadic wind using CFD model. Wind Struct. 26, 369–382.

Yuan, F., Guirong, Y., Honerkamp, R., Isaac, K.M., Ruoqiang, F., 2016. Effects of chamber shape on simulation of tornado-like flow in a laboratory. In: Mousaad Aly, A., Dragomirescu, E. (Eds.), Wind Engineering for Natural Hazards-Modeling, Simulation, and Mitigation of Windstorm Impact on Critical Infrastructure. ASCE, Reston, VA.

Yuan, F., Yan, G., Honerkamp, R., Kakkattukuzhy, M.I., Zhao, M., Mao, X., 2019. Numerical simulation of laboratory tornado simulator that can produce translating tornado-like wind flow. J. Wind Eng. Ind. Aerod. 190, 200–217.